HHS Public Access

Author manuscript

Sci Transl Med. Author manuscript; available in PMC 2023 January 24.

Published in final edited form as:

Sci Transl Med. 2022 August 17; 14(658): eabj2681. doi:10.1126/scitranslmed.abj2681.

Sphingosine 1-phosphate signaling in perivascular cells enhances inflammation and fibrosis in the kidney

Shinji Tanaka[1,2], **Shuqiu Zheng**[1], **Yugesh Kharel**[3], **Russell G. Fritzemeier**[4], **Tao Huang**[3], **Daniel Foster**[4], **Nabin Poudel**[1], **Eibhlin Goggins**[1], **Yusuke Yamaoka**[1], **Kinga P. Rudnicka**[1], **Jonathan E. Lipsey**[1], **Hope V. Radel**[1], **Sophia M. Ryuh**[1], **Tsuyoshi Inoue**[1], **Junlan Yao**[1], **Diane L. Rosin**[3], **Susan R. Schwab**[5], **Webster L. Santos**[4], **Kevin R. Lynch**[3], **Mark D. Okusa**[1,*]

[1]Division of Nephrology and Center for Immunity, Inflammation, and Regenerative Medicine, University of Virginia, Charlottesville, Virginia 22903, USA.

[2]Division of Nephrology and Endocrinology, University of Tokyo Graduate School of Medicine, Tokyo 113-8655, Japan.

[3]Department of Pharmacology, University of Virginia, Charlottesville, Virginia 22903, USA.

[4]Department of Chemistry and Center for Drug Discovery, Virginia Tech, Blacksburg, Virginia 24061, USA.

[5]Skirball Institute of Biomolecular Medicine, New York University Grossman School of Medicine, NY, New York 10016, USA.

Abstract

Chronic kidney disease (CKD), characterized by sustained inflammation and progressive fibrosis, is highly prevalent and can eventually progress to end-stage kidney disease. However, current treatments to slow CKD progression are limited. Sphingosine 1-phosphate (S1P), a product of sphingolipid catabolism, is a pleiotropic mediator involved in many cellular functions, and drugs targeting S1P signaling have previously been studied particularly for autoimmune diseases. The primary mechanism of most of these drugs is functional antagonism of S1P receptor-1 (S1P1) expressed on lymphocytes and the resultant immunosuppressive effect. Here, we documented the role of local S1P signaling in perivascular cells in the progression of kidney fibrosis using primary kidney perivascular cells and several conditional mouse models. S1P was predominantly produced by sphingosine kinase 2 in kidney perivascular cells and exported via spinster homolog 2 (Spns2). It bound to S1P1 expressed in perivascular cells to enhance production of proinflammatory

*Corresponding author. mdo7y@virginia.edu.

Author contributions: S.T., Y.K., D.L.R., K.R.L., and M.D.O. designed research studies. W.L.S., R.G.F., and D.F. designed and synthesized the Spns2 inhibitor. S.R.S. provided *Spns2*$^{fl/fl}$ mice. S.T., S.Z., Y.K., T.H., N.P., E.G., Y.Y., K.P.R., J.E.L., H.V.R., S.M.R., T.I., and J.Y. conducted experiments and acquired and analyzed data. S.T., D.L.R., K.R.L., and M.D.O. wrote the manuscript.

SUPPLEMENTARY MATERIALS

www.science.org/doi/10.1126/scitranslmed.abj2681

Competing interests: Y.K., R.G.F., D.F., W.L.S., and K.R.L. have patent applications for the Spns2 inhibitor compounds [K.R.L., Y.K., W.L.S., R.G.F., D.F., and A. Peralta; "Inhibitors of spinster homolog 2 (SPNS2) for use in therapy"; U.S. patent 63/076,105; filed 9 September 2020]. All other authors declare that they have no competing interests.

Data and materials availability: All data associated with this study are present in the paper or the Supplementary Materials. SLF1081851 is available via material transfer agreement on request to K.R.L.

cytokines/chemokines upon injury, leading to immune cell infiltration and subsequent fibrosis. A small-molecule Spns2 inhibitor blocked S1P transport, resulting in suppression of inflammatory signaling in human and mouse kidney perivascular cells in vitro and amelioration of kidney fibrosis in mice. Our study provides insight into the regulation of inflammation and fibrosis by S1P and demonstrates the potential of Spns2 inhibition as a treatment for CKD and potentially other inflammatory and fibrotic diseases that avoids the adverse events associated with systemic modulation of S1P receptors.

INTRODUCTION

Chronic kidney disease (CKD) is a condition characterized by deterioration of kidney function with sustained inflammation and progressive fibrosis in the kidneys that affects nearly 10% of the population worldwide (1, 2). CKD is a major public health problem because it can eventually progress to end-stage kidney disease, which requires dialysis or kidney transplantation, and it is also a strong risk factor for cardiovascular disease (3, 4). The precise mechanisms of CKD progression remain poorly understood, and current treatments to slow CKD progression are limited and nonspecific (5). Consequently, the outcomes in patients with CKD remain poor (6).

Sphingosine 1-phosphate (S1P), a product of cell membrane sphingolipid catabolism, is a pleiotropic mediator involved in a variety of cellular functions such as adhesion, migration, inflammation, and proliferation in many cell types (7-9). S1P is generated from sphingosine intracellularly by sphingosine kinases 1 and 2 (SphK1 and SphK2). S1P is exported from cells by spinster homolog 2 (Spns2) (10) or major facilitator superfamily 2b (Mfsd2b) (11) and acts on five G protein–coupled S1P receptors, S1P1 to S1P5, to affect various cellular functions. S1P signaling is a validated drug target: Fingolimod (FTY720), which is an S1P1, S1P3, S1P4, and S1P5 agonist, was approved in 2010 by the U.S. Food and Drug Administration as the first oral drug for treatment of relapsing-remitting multiple sclerosis (12, 13). Fingolimod induces sustained internalization and degradation of lymphocyte S1P1, resulting in decreased S1P1 expression (14). Because sensing the S1P gradient between the lymph and secondary lymphoid organs via S1P1 is critical for lymphocyte egress into lymphatic circulation (15), S1P receptor modulators such as fingolimod inhibit the egress of auto-reactive lymphocytes from secondary lymphoid organs and suppress their migration into the inflamed tissue to slow the progression of autoimmune diseases.

Fingolimod has also been investigated as a treatment for kidney diseases. The drug is effective against acute kidney injury (AKI) (16-18) and kidney fibrosis (19, 20) in different animal models. However, fingolimod failed in late-stage clinical trials of kidney transplantation due to decreased graft function and increased rates of adverse effects compared with standard care (21-23). Serious adverse effects of fingolimod include initial dose bradycardia and, infrequently, macular edema. The former is due to the initial agonistic effect of fingolimod on S1P1, resulting in activation of the G protein–coupled inwardly rectifying potassium channels on atrial myocytes (24), whereas the latter has been ascribed to decreased vascular barrier function by functional antagonism of endothelial S1P1 (25). Thus, alternative strategies are desirable for the development of drugs targeting S1P

signaling for patients with kidney disease. One such strategy is inhibition of SphK2. Our group and others have shown that *Sphk2*$^{-/-}$ or wild-type mice treated with an SphK2 inhibitor were protected against kidney fibrosis (26, 27); however, the mechanism whereby SphK2 contributes to the progression of kidney fibrosis—and why its blockade is protective — remain uncertain.

Bone marrow chimera studies have suggested that *Sphk2* deletion in kidney resident cells contributes to the protection against kidney fibrosis in *Sphk2*$^{-/-}$ mice (27). Thus, we hypothesized that SphK2 in proximal tubular epithelial cells or perivascular cells (pericytes/fibroblasts) contributes to kidney fibrosis progression, because those populations play a critical role in this context (28, 29). In the current study, our results in conditional mouse models suggested that SphK2 in kidney perivascular cells is important for the progression of kidney fibrosis. In vitro, both genetic ablation and inhibition of SphK2 suppressed production and release of proinflammatory cytokines/chemokines from primary mouse kidney perivascular cells when they were stimulated with Toll-like receptor 2/4 (TLR2/4) agonists or damage-associated molecular patterns (DAMPs) released from injured kidneys. Furthermore, we identified Spns2 as the S1P transporter expressed in kidney perivascular cells and found that S1P in the extracellular space binds to S1P1 expressed in these cells to enhance inflammatory signaling on injury. We also used a small-molecule inhibitor of Spns2 that suppressed inflammatory signaling in kidney perivascular cells in vitro and ameliorated kidney fibrosis in vivo. The anti-inflammatory effect of SphK2 inhibition and Spns2 inhibition was recapitulated in primary human kidney perivascular cells.

Together, we demonstrated that the SphK2/S1P/Spns2/S1P1 axis enhanced inflammatory signaling in perivascular cells after injury, which aggravated immune cell infiltration and subsequent fibrosis in the mouse kidney. Our study provides insight into the regulation of inflammation and fibrosis by S1P and suggests that Spns2 inhibition could be a promising therapy for the treatment of kidney fibrosis and potentially other inflammatory and fibrotic diseases.

RESULTS

SphK2 in kidney perivascular cells plays an important role in the progression of kidney fibrosis

Proximal tubular epithelial cells and perivascular cells (pericytes/fibroblasts) play a critical role in the progression of kidney fibrosis (28, 29). To investigate the contribution of SphK2 in proximal tubule and perivascular cells to the progression of kidney fibrosis, we crossed *Sphk2*^{flox} mice (30) with *Pepck-Cre* (31) and *Foxd1-Cre* (29) mice to selectively delete *Sphk2* in proximal tubular epithelial cells and perivascular cells in the kidney, respectively. First, *Pepck-Cre;Sphk2*$^{fl/fl}$ (*Sphk2*^{PTECKO}) mice and Cre-negative littermate controls (*Sphk2*^{PTECWT}) (fig. S1, A and B) were subjected to unilateral (left) kidney ischemia-reperfusion injury (IRI), followed by contralateral (right) nephrectomy on day 13, and collection of the IRI (left) kidney and blood on day 14 (fig. S1C). IRI kidneys of *Sphk2*^{PTECWT} and *Sphk2*^{PTECKO} mice had the same extent of increased collagen deposition as assessed by Masson's trichrome (fig. S1D) and picrosirius red staining (fig. S1E) compared with sham-operated kidneys. Transcription expression of fibrosis markers *Acta2*

[α–smooth muscle actin (αSMA)], *Col1a1* (collagen type I α1 chain), and *Col3a1* (collagen type III α1 chain) was also increased in IRI kidneys of *Sphk2*^{PTECWT} and *Sphk2*^{PTECKO} mice to a similar degree (fig. S1F). Furthermore, elevated plasma creatinine concentrations were similar in *Sphk2*^{PTECWT} and *Sphk2*^{PTECKO} mice (fig. S1G). Together, these results demonstrated that SphK2 in proximal tubular epithelial cells does not play an important role in the progression of kidney fibrosis.

Next, we investigated a potential role of SphK2 in kidney perivascular cells (fibroblasts/pericytes) in the progression of kidney fibrosis using *Foxd1-Cre;Sphk2*$^{fl/fl}$ (*Sphk2*^{PVCKO}) mice and littermate controls (*Sphk2*^{PVCWT}) (fig. S2, A to E). In the unilateral kidney IRI model (Fig. 1A), kidney fibrosis was ameliorated in *Sphk2*^{PVCKO} mice compared with *Sphk2*^{PVCWT} mice as shown by decreased collagen deposition (Fig. 1, B and C) with a decrease in expression of fibrosis markers (Fig. 1D) and in plasma creatinine concentrations (Fig. 1E).

Immune cells have a critical role in the progression of kidney fibrosis, and the protective effects of fingolimod in kidney fibrosis suggest that impairing S1P generation and signaling in these cells affect kidney outcomes (19, 20). We therefore sought to determine the specificity of *Foxd1-Cre* to the perivascular compartment and specifically to exclude the possibility that *Foxd1-Cre* was expressed in immune cells. We confirmed that Cre recombination did not occur in the bone marrow cells of *Sphk2*^{PVCKO} mice (fig. S3). We also subjected *Pdgfr*β-*CreERT2;Sphk2*$^{fl/fl}$ mice to unilateral IRI. Platelet-derived growth factor receptor-β is another established marker of perivascular cells with no expression in immune cells in adult mice (32, 33), and *Pdgfr*β-*CreERT2* mice have been previously validated (34-36). *Pdgfr*β-*CreERT2;Sphk2*$^{fl/fl}$ mice showed attenuated kidney fibrosis compared with littermate control mice (fig. S4, A to C), recapitulating the phenotype of *Foxd1-Cre;Sphk2*$^{fl/fl}$ mice subjected to unilateral IRI-induced fibrosis. We further confirmed that neither plasma S1P concentrations (fig. S5A) nor the number of immune cells (B cells, $CD4^+$/$CD8^+$ T cells, and monocytes) in peripheral blood (fig. S5B) was different between *Sphk2*^{PVCWT} and *Sphk2*^{PVCKO} mice. The spleen (fig. S5, C and D) and inguinal lymph nodes (fig. S5, E and F) also showed no difference in terms of weight and fraction of immune cells (B cells, $CD4^+$/$CD8^+$ T cells, macrophages, and monocytes). The gating strategy is shown in fig. S6 (A and B). Last, staining of perivascular and endothelial cells excluded the possibility that the protection against kidney fibrosis in *Sphk2*^{PVCKO} mice was attributed to alterations in vascular patterning at baseline (fig. S2, D and E). Together, these findings suggested an important role for SphK2 in kidney perivascular cells, not in immune cells, in IRI-induced kidney fibrosis.

The severity of the initial episode(s) of AKI is closely correlated with the extent of kidney fibrosis (CKD) that subsequently develops in animal models, such as after kidney IRI (37) and folic acid injection (38), and in humans (39, 40). Thus, we investigated whether the reduced kidney fibrosis in *Sphk2*^{PVCKO} mice in the unilateral IRI model was attributed to reduced kidney injury in the acute phase of IRI. In a bilateral kidney IRI model (fig. S7A), *Sphk2*^{PVCKO} mice showed the same severity of AKI [as assessed by histological injury score (fig. S7B), *Havcr1* (kidney injury molecule-1, a representative marker of tubular injury) expression in the kidney (fig. S7C), and plasma creatinine concentrations (fig. S7D)] as

Sphk2^{PVCWT} mice. There was also no difference in kidney *Havcr1* expression at 24 hours in the unilateral IRI model between these two genotypes (fig. S7, E and F). These findings demonstrated that *Sphk2* deletion in kidney perivascular cells ameliorates IRI-induced kidney fibrosis without affecting the severity of kidney injury in the acute phase.

We further confirmed the role of SphK2 in kidney perivascular cells in the progression of kidney fibrosis with the folic acid model of kidney fibrosis. Injection of folic acid (250 mg/kg) into mice induces AKI and subsequent kidney fibrosis (27). Consistent with the unilateral IRI model, at 14 days after folic acid injection (Fig. 2A), *Sphk2*^{PVCKO} mice exhibited a reduced kidney fibrosis than *Sphk2*^{PVCWT} mice, as shown by decreased collagen deposition (Fig. 2, B and C), lower transcriptional expression of fibrosis markers (Fig. 2D), and lower blood urea nitrogen (BUN) concentrations (Fig. 2E). Folic acid injection did not increase plasma creatinine at day 14 [0.10 ± 0.05 mg/dl (*Sphk2*^{PVCWT}/vehicle, $n = 4$) versus 0.07 ± 0.03 mg/dl (*Sphk2*^{PVCKO}/vehicle, $n = 4$) versus 0.11 ± 0.01 mg/dl (*Sphk2*^{PVCWT}/folic acid, $n = 13$) versus 0.12 ± 0.02 mg/dl (*Sphk2*^{PVCKO}/folic acid, $n = 11$)]. In contrast, at 24 hours after folic acid injection (fig. S8A), *Sphk2*^{PVCKO} mice showed a similar severity of AKI compared with *Sphk2*^{PVCWT} mice based on histology (fig. S8B), *Havcr1* expression in the kidney (fig. S8C), and plasma creatinine concentrations (fig. S8D). In another subset of mice, no difference in plasma creatinine was observed on day 2 (0.44 ± 0.14 mg/dl versus 0.49 ± 0.19 mg/dl) and day 3 (0.41 ± 0.18 mg/dl versus 0.38 ± 0.04 mg/dl) between *Sphk2*^{PVCWT} versus *Sphk2*^{PVCKO} mice ($n = 4$ to 6). Together, the data from the two AKI/CKD models suggested that SphK2 expressed in perivascular cells contributed to the progression of kidney fibrosis.

SphK2 enhances inflammatory signaling in kidney perivascular cells on injury and promotes macrophage infiltration and fibrosis in the kidney

To investigate the mechanism by which SphK2 in perivascular cells contributes to the progression of kidney fibrosis, primary perivascular cells were isolated from the kidneys of *Sphk2*^{PVCWT} and *Sphk2*^{PVCKO} mice. At baseline, *Sphk2* showed greater transcription than *Sphk1* (18.1 ± 3.6 times, $n = 5$ each) in primary wild-type kidney perivascular cells, and *Sphk2*-deficient perivascular cells had lower concentrations of S1P in cells and media than wild-type cells (Fig. 3A). Because kidney perivascular cells are the major source of myofibroblasts in fibrotic kidneys (29), *Sphk2* deletion in kidney perivascular cells could prevent transdifferentiation into myofibroblasts and be responsible for the attenuation of kidney fibrosis observed in *Sphk2*^{PVCKO} mice. However, genetic deletion (fig. S9A) or pharmacological inhibition (SLM6031434) (fig. S9B) (41) of *Sphk2* in primary kidney perivascular cells did not affect αSMA expression, suggesting that transdifferentiation into myofibroblasts was not affected. Perivascular cells are also major innate immune sentinels in the kidney and produce proinflammatory cytokines/chemokines on injury in a TLR2/4-dependent manner to promote immune cell infiltration (especially monocytes/macrophages) (42, 43), leading to persistent inflammation and progression of kidney fibrosis (44). Thus, we hypothesized that *Sphk2* deletion suppresses inflammatory signaling in kidney perivascular cells, resulting in less kidney immune cell infiltration and ameliorated fibrosis. SphK2 but not SphK1 was up-regulated in kidney perivascular cells by treatment with lipopolysaccharide (LPS) (Fig. 3B and fig. S10A) or by IRI (fig. S10, B and C),

indicating that SphK2 may be involved in injury-induced inflammatory signaling in these cells. Consistent with our hypothesis, LPS stimulation resulted in increased transcription of proinflammatory cytokines and chemokines (*Ccl2*, *Il6*, *Cxcl1*, and *Cxcl2*) in perivascular cells, and this response was suppressed in *Sphk2*-deficient cells (Fig. 3C). We also stimulated cells with TLR2 agonists and kidney DAMPs released from injured kidneys [obtained by collecting extracellular molecules 24 hours after unilateral IRI (42, 45)]; *Sphk2* deficiency suppressed inflammatory transcript expression induced by these stimuli (Fig. 3D). We further confirmed these findings by using enzyme-linked immunosorbent assay (ELISA) and found suppressed secretion of monocyte chemoattractant protein-1 (MCP-1), interleukin-6 (IL-6), and CXCL-1 from *Sphk2*-deficient cells (Fig. 3E). Nuclear factor κB (NF-κB) activation induced by LPS treatment was suppressed in *Sphk2*-deficient cells (Fig. 3F), possibly explaining the decreased production of proinflammatory cytokines and chemokines in these cells. In contrast, transcription and secretion of those proinflammatory molecules induced by LPS treatment were not different between primary tubular epithelial cells isolated from intact $Sphk2^{PVCWT}$ and $Sphk2^{PVCKO}$ mice (fig. S11, A and B). This result suggested that *Sphk2* deletion in kidney perivascular cells did not affect inflammatory signaling in adjacent tubular epithelial cells on injury. Furthermore, treatment of wild-type kidney perivascular cells with a selective SphK2 inhibitor [SLM6031434 (41)] before LPS treatment recapitulated the phenotype of *Sphk2*-deficient cells (Fig. 3G). Pharmacological inhibition of SPHK2, the predominant isoform in human perivascular cells (fig. S12A), reduced S1P in the supernatant (fig. S12B) as well as transcription and secretion of proinflammatory molecules induced by treatment with TLR2/4 agonists (fig. S12, C and D) in primary human kidney perivascular cells. Together, these results suggested that SphK2 enhanced inflammatory signaling in primary kidney perivascular cells when stimulated with TLR2/4 agonists or kidney DAMPs.

To confirm that SphK2 enhanced inflammatory signaling after injury in kidney perivascular cells in vivo, perivascular cells were isolated from IRI kidneys of $Sphk2^{PVCWT}$ and $Sphk2^{PVCKO}$ mice, and mRNA was immediately extracted and analyzed. Kidney IRI increased the expression of proinflammatory cytokines and chemokines in perivascular cells, and this response was suppressed in $Sphk2^{PVCKO}$ mice (fig. S13A), consistent with the results of ex vivo stimulation with TLR2/4 agonists and kidney DAMPs (Fig. 3, C and D). Less macrophage infiltration was seen in IRI kidneys of $Sphk2^{PVCKO}$ mice compared with $Sphk2^{PVCWT}$ mice (fig. S13B), confirming suppression of inflammatory signaling in $Sphk2^{PVCKO}$ mice (42).

To investigate the contribution of suppressed inflammatory signaling in kidney perivascular cells and decreased macrophage infiltration in the kidney to ameliorated kidney fibrosis in $Sphk2^{PVCKO}$ mice, we depleted phagocytic monocytes and macrophages with liposome clodronate beginning 2 days after unilateral IRI (fig. S14A). We previously showed that monocyte and macrophage depletion with this protocol ameliorated kidney fibrosis in the same model (46). As expected, treatment with liposome clodronate ameliorated kidney fibrosis with suppressed macrophage infiltration in $Sphk2^{PVCWT}$ mice, whereas there was no additional effect of *Sphk2* deletion in perivascular cells in macrophage-depleted mice (fig. S14, B to F). These results showed that *Sphk2* deletion in kidney perivascular cells

ameliorated kidney fibrosis through suppression of perivascular cell inflammatory signaling and kidney macrophage infiltration.

S1P/S1P1 signaling mediates inflammatory response in perivascular cells

Next, we hypothesized that S1P produced and secreted by kidney perivascular cells binds to its receptors expressed in perivascular cells to enhance inflammatory signaling. S1P supplementation to the medium of *Sphk2*-deficient cells almost completely reconstituted the proinflammatory cytokine response to LPS (Fig. 4A), further supporting our hypothesis. Next, we sought to identify which receptor(s) among S1P1 to S1P5 play a critical role. Kidney perivascular cells expressed *S1pr1/2*/3 (Fig. 4B), and this pattern was conserved in human cells (fig. S15A). Knockdown of *S1pr1*, but not *S1pr2* or *S1pr3* (fig. S15B), suppressed proinflammatory cytokine/chemokine production in LPS-treated wild-type cells (Fig. 4C), whereas these effects were not observed in *Sphk2*-deficient cells (Fig. 4D). S1P supplementation to the medium of *Sphk2*-deficient cells enhanced the inflammatory response to LPS, and *S1pr1* knockdown almost completely blocked the effect of S1P supplementation (Fig. 4E), further supporting the role of the SphK2/S1P/S1P1 axis in enhancing inflammatory signaling. To confirm the importance of S1P/S1P1 signaling in kidney perivascular cells in vivo, we crossed $S1pr1^{flox}$ mice (47) with *Foxd1-Cre* mice to selectively delete *S1pr1* in perivascular cells in the kidney, and $Foxd1\text{-}Cre;S1pr1^{fl/fl}$ ($S1pr1^{PVCKO}$) mice and Cre-negative littermate controls ($S1pr1^{PVCWT}$) were subjected to unilateral kidney IRI (Fig. 5A). $S1pr1^{PVCKO}$ mice showed amelioration of kidney fibrosis compared with control mice, as demonstrated by the decrease in collagen deposition (Fig. 5, B and C), expression of fibrosis markers (Fig. 5D), and plasma creatinine concentrations (Fig. 5E), accompanied by suppressed macrophage infiltration (Fig. 5F), recapitulating the phenotype of $Sphk2^{PVCKO}$ mice. Together, these results suggested that S1P, predominantly produced by SphK2 in kidney perivascular cells, was transported into the extracellular space and then bound to S1P1 expressed in perivascular cells to enhance inflammatory signaling on injury.

Spns2 exports S1P from perivascular cells and Spns2 inhibition suppresses inflammatory response and ameliorates kidney fibrosis

Last, we investigated whether the S1P exporter expressed in kidney perivascular cells enables “inside-out” signaling of S1P. Spns2 was expressed in primary kidney perivascular cells in mice (Fig. 6A) and humans (fig. S16A), and genetic knockdown of *Spns2* (fig. S16B) decreased S1P in the medium (Fig. 6B), suggesting that Spns2 is an S1P exporter in these cells. Treatment with LPS up-regulated *Spns2* expression in perivascular cells (Fig. 6C). This is consistent with recent single-cell RNA sequencing data of mouse injured kidneys showing robust *Spns2* expression in activated fibroblasts (48) and implies an involvement of Spns2 in the inflammatory response in these cells. Knockdown of *Spns2* expression suppressed the inflammatory response to LPS in wild-type cells and S1P supplementation to the medium almost completely blocked the suppression (Fig. 6D). *S1pr1* knockdown in the setting of *Spns2* knockdown and S1P supplementation suppressed the inflammatory response as well (Fig. 6D). These results suggested the inside-out signaling cascade involving SphK2, S1P, Spns2, and S1P1. To explore further the role of Spns2 in kidney perivascular cells in vivo, we crossed $Spns2^{flox}$ mice (49) with *Foxd1-Cre* mice to

delete *Spns2* in kidney perivascular cells selectively, and *Foxd1-Cre;Spns2*$^{fl/fl}$ (*Spns2*^{PVCKO}) mice and Cre-negative littermate controls (*Spns2*^{PVCWT}) were subjected to unilateral kidney IRI (Fig. 6E). *Spns2*^{PVCKO} mice showed decreased collagen deposition (Fig. 6F) and lower plasma creatinine concentrations (Fig. 6G) in IRI kidneys compared with control mice.

Because our observations suggested that S1P exported via Spns2 is an initial step in the inside-out signaling of S1P in kidney perivascular cells to enhance inflammatory response, Spns2 may be a drug target candidate. To explore this idea, we used a small-molecule Spns2 inhibitor [SLF1081851 (50) and fig. S17A] that evokes dose-dependent peripheral blood lymphocytopenia and a decrease in plasma S1P in mice (fig. S17, B and C), which is consistent with the phenotype of *Spns2*-deficient mice (49). Further, the compound is devoid of S1P1 agonist activity and its half-maximal inhibitory concentration (IC_{50}) for release of S1P from U-937 monocytes is about 1 μM (fig. S17D). In mouse primary kidney perivascular cells, SLF1081851 inhibited S1P export in a concentration-dependent manner, as demonstrated by decreased S1P concentrations in the medium, whereas S1P intracellular concentrations were not affected (Fig. 7A) [in contrast to decreased S1P intracellular concentrations in *Sphk2*-deficient cells (Fig. 3A)]. Further, SLF1081851 treatment inhibited the inflammatory response to LPS in perivascular cells (Fig. 7B). In human perivascular cells, SLF108151 reduced inflammatory response to LPS measured by reduction in the production of proinflammatory cytokines/chemokines (fig. S17E), suggesting that the Spns2-mediated inflammatory response is conserved between mouse and human. To determine whether SLF1081851 was efficacious in vivo, wild-type mice underwent kidney unilateral IRI (day 0) and were administered either SLF1081851 (5 or 10 mg/kg) or vehicle intraperitoneally once daily from day 4 to day 13, followed by contralateral nephrectomy at day 13 and euthanasia at day 14 (Fig. 7C). This delayed administration of the inhibitor was intended to avoid potential effects on the acute phase of IRI. SLF1081851 treatment decreased collagen deposition in the kidney (Fig. 7D) and decreased plasma creatinine (Fig. 7E) in a dose-dependent manner. We also tested fingolimod in the same unilateral IRI model. First, dose-response data showed that fingolimod at doses as low as 0.03 mg/kg caused profound lymphopenia (fig. S18A). Fingolimod treatment, at 0.1 or 1 mg/kg, failed to protect from kidney fibrosis as assessed by collagen deposition in the kidney and plasma creatinine (fig. S18, B to D). Further, SLF1081851 was protective against kidney fibrosis in the folic acid model, as demonstrated by kidney collagen deposition and BUN (fig. S19, A to C). Administration of SLF1081851 did not affect body weight or plasma aspartate aminotransferase (AST) and alanine aminotransferase (ALT) concentrations in the unilateral IRI model (fig. S19, D and E) or the folic acid model (fig. S19, F and G).

DISCUSSION

Here, we present evidence for the important pathological role of local S1P signaling in perivascular cells in the progression of kidney fibrosis—S1P produced by SphK2 in kidney perivascular cells is transported into the extracellular space through Spns2 and then binds to S1P1 expressed in perivascular cells to enhance production and release of proinflammatory cytokines/chemokines on injury, leading to infiltration of immune cells and subsequent fibrosis (fig. 20). Current models of immune cell regulation by S1P signaling emphasize direct interaction between S1P and S1P receptors expressed on immune cells, but our data

suggest that S1P signaling in perivascular cells indirectly regulates immune cell recruitment and kidney fibrosis.

Our results suggest that export of S1P from kidney perivascular cells and its binding to S1P1 expressed on perivascular cells enhance inflammatory response and fibrosis progression. S1P exported from perivascular cells could also affect other adjacent cells such as endothelial cells, tubular epithelial cells, and immune cells in a paracrine manner. However, S1P/S1P1 signaling has been shown to be protective in endothelial cells (51), which is not consistent with the protective phenotype observed when S1P/S1P1 signaling is disrupted in *Sphk2*^{PVCKO} and *Spns2*^{PVCKO} mice. In this study, we also showed that LPS-induced inflammatory response in primary tubular epithelial cells isolated from *Sphk2*^{PVCWT} and *Sphk2*^{PVCKO} mice was comparable, making it unlikely that *Sphk2* deletion in kidney perivascular cells modulated inflammatory signaling in adjacent tubular epithelial cells to confer protection. The function, localization, and survival of immune cells are also regulated by S1P signaling (8). Pericytes in the thymus release S1P, which interacts with S1P1 expressed in thymocytes to promote T cell egress from thymus (52). However, it is unlikely that S1P exported from kidney perivascular cells directly affects the infiltration of immune cells from circulation because immune cells in circulation have been exposed to high concentrations of S1P and therefore may be desensitized to S1P. It is possible that S1P exported from perivascular cells could affect immune cells that have infiltrated into the injured kidney and resensitized to S1P or resident immune cells. However, *S1pr1*^{PVCKO} mice showed protection against kidney fibrosis with suppressed macrophage infiltration, which recapitulated the phenotype of *Sphk2*^{PVCKO} and *Spns2*^{PVCKO} mice, suggesting that S1P/S1P1 signaling in kidney perivascular cells contributes to the progression of kidney fibrosis. The molecular mechanism of this highly localized regulation of S1P/S1P1 signaling in kidney perivascular cells is yet to be determined.

The salient mechanism of action of fingolimod (and other S1P receptor modulators) is functional antagonism of the S1P1 receptor, which is expressed on lymphocytes. With fingolimod treatment, lymphocytes cannot sense the high S1P environment of efferent lymph/blood and thus cannot egress properly from secondary lymphoid tissues, resulting in peripheral blood lymphopenia. Mouse genetic studies indicate that lymph S1P is extruded from lymph endothelium via Spns2 (49). Thus, it is possible that Spns2 inhibitors, by flattening the lymph S1P gradient, may recapitulate the effects of S1P receptor modulators. Although a definitive answer to this issue awaits the discovery of a suite of high quality Spns2 inhibitors, initial results indicate some curious inconsistencies. For example, Spns2 inhibition blocks egress of lymphocytes from lymph nodes (directed by lymph S1P) but does not affect egress of lymphocytes from the spleen (directed by blood S1P), which is probably due to a modest decrease in blood S1P concentrations with Spns2 inhibition (49, 53), whereas fingolimod treatment blocks egress of lymphocytes from both compartments. S1P receptor modulator class adverse events such as first-dose bradycardia and macular edema, which are via S1P1 receptors on myocytes and retinal endothelial cells, respectively, might be lessened because Spns2 inhibitors do not directly act on S1P1 receptors and cause only a modest decrease in blood S1P concentrations. There was no difference in lung vascular permeability between endothelial *Spns2* knockout mice and littermate controls, whereas fingolimod treatment increased lung vascular permeability (49). Our results also showed

that SLF1081851, but not fingolimod, protected against kidney fibrosis in the unilateral IRI model. The inconsistency with previous studies that showed beneficial effects of fingolimod in kidney fibrosis may be due to different models and perhaps, more importantly, different fingolimod administration protocols. Administration of SLF1081851 or fingolimod started 4 days after IRI surgery in our protocol, whereas fingolimod administration started on the same day of surgery in previous studies (20). With the latter protocol, ameliorated fibrosis may be due to the protective effects of fingolimod on AKI, which has been previously shown (16). Furthermore, our protocol (administration starting at day 4) is more clinically relevant. Thus, although there is a concern about Spns2 blockade [for example, worsened hypertension and cardiac hypertrophy in mice with endothelial *Spns2* deletion (54)], these findings suggest that Spns2 inhibitors might be promising in renal disease.

Our data show a proinflammatory role of the SphK2/S1P/Spns2/S1P1 axis in perivascular cells. This is consistent with recent findings that Spns2 expressed in brain microglia (55) and proximal tubular epithelial cells (56) enhances proinflammatory cytokine/chemokine expression in vitro. On the other hand, S1P1 signaling has been shown to be tissue-protective and anti-inflammatory in endothelial cells. Endothelial S1P1 signaling maintains tight junctions to promote barrier function (51) and suppresses endothelial expression of the leukocyte adhesion molecules (intercellular adhesion molecule–1 and vascular cell adhesion molecule–1) (57-59). The consequences of S1P1 signaling seem to depend highly on cell type; S1P1 signaling up-regulates production of proinflammatory cytokines/chemokines in macrophages (60-63), astrocytes (64), and melanoma cells (65). Overexpression of *S1pr1* in cardiac fibroblasts enhances cardiac fibrosis in vivo and increases production of IL-6 in vitro (66). It is still not known what causes the different consequences of S1P1 signaling in different cell types. S1P1 signaling is intricately regulated by many factors—β-arrestin coupling, receptor modulators, and endocytosis. These factors might contribute to cell type–specific changes induced by S1P1 activation.

Limitations of our work include the uncertainty about the transferability of the importance of the SphK2/S1P/Spns2/S1P1 axis from animals to humans. Although we show the data of primary human kidney perivascular cells, future studies need to confirm the importance of this axis using human kidney tissue. Another limitation is that the effect of pharmacological Spns2 inhibition was examined by a single molecule. Testing multiple, well-characterized Spns2 inhibitors with distinct chemical scaffolds would be warranted to mitigate a risk of off-target effects.

In summary, our study provides evidence for S1P-mediated regulation of inflammatory signaling in renal perivascular cells. Targeting this S1P signaling pathway, enabling control of S1P concentrations in the local microenvironment, is a promising strategy for the treatment of kidney fibrosis and potentially other inflammatory and fibrotic diseases that can perhaps avoid the adverse events associated with systemic modulation of S1P receptors.

MATERIALS AND METHODS

Study design

The objective of this study was to determine how SphK2 contributes to the progression of kidney fibrosis and how blockade of SphK2 might be protective. We hypothesized that SphK2 in kidney perivascular cells plays an important role in the progression of kidney fibrosis. To test this hypothesis, we designed a study using several models of kidney injury in mice in which *Sphk2* was deleted in kidney perivascular cells or in proximal tubular epithelial cells. Next, we performed in vitro experiments using primary perivascular cells isolated from mouse kidneys and primary human kidney perivascular cells purchased from Cell Biologics to show that SphK2 in perivascular cells enhances inflammatory signaling on injury. Then, we hypothesized that S1P signaling (SphK2/S1P/Spns2/S1P1 axis) in perivascular cells is critical in this context. To test this hypothesis, we designed a study using mouse and human primary kidney perivascular cells and mice in which *S1pr1 or Spns2* was deleted in kidney perivascular cells. Last, to explore the idea that Spns2 is a potential drug target, we used a small-molecule Spns2 inhibitor (SLF1081851) in in vitro (mouse and human primary kidney perivascular cells and U-937 cells) and in vivo (wild-type mice) experiments. Sample sizes were determined on the basis of previous pilot and published experiments (27, 46). The number of biological replicates is indicated in the figure legends. No data were excluded from the analysis. Animal experiments were performed using littermates, which facilitates appropriate randomization. Within the littermate groups, animals were selected at random for each experimental group (IRI or sham surgeries). IRI surgeries were performed by an operator masked to experimental settings and to the mouse genotype. Plasma creatinine and BUN measurements and histological analyses were performed by investigators masked to experimental setting.

Study approval

All animal procedures were performed in adherence to the National Institutes of Health (NIH) *Guide for the Care and Use of Laboratory Animals*. All animal protocols were approved by the University of Virginia Institutional Animal Care and Use Committee.

Animals

Male mice (8 to 12 weeks of age) were used for all experiments except for the experiments to determine the effect of SLF1081851 on blood lymphocytes and plasma S1P concentrations (described below). Mice with a floxed *Sphk2* allele (*Sphk2*^{flox} mice; exons 4 to 6 flanked by loxP sites) were made under contract by Ingenious Targeting Laboratories on a C57BL/6 background (30). *Pepck-Cre* mice provided by V. Haase (Vanderbilt University) (31) were crossed with *Sphk2*$^{fl/fl}$ mice. The *Pepck*$^{Cre/+}$ *Sphk2*$^{fl/+}$ progeny were crossed with *Sphk2*$^{fl/fl}$ mice to obtain *Pepck*$^{Cre/+}$ *Sphk2*$^{fl/fl}$ mice, which were then crossed with *Sphk2*$^{fl/fl}$ mice to generate the *Pepck-Cre;Sphk2*$^{fl/fl}$ (*Sphk2*^{PTECKO}) mice and the littermate control *Sphk2*$^{fl/fl}$ (*Sphk2*^{PTECWT}) mice. Similarly, *Foxd1-Cre;Sphk2*$^{fl/fl}$ (*Sphk2*^{PVCKO}), *Foxd1-Cre;S1pr1*$^{fl/fl}$ (*S1pr1*^{PVCKO}), *Foxd1-Cre;Spns2*$^{fl/fl}$ (*Spns2*^{PVCKO}), and *Pdgfr*β-*CreERT2;Sphk2*$^{fl/fl}$ mice and their littermate controls were generated by crossing *Foxd1*$^{tm1(GFP/cre)Amc}$/*J*(*Foxd1-Cre*) (29) or *Pdgfr*β-*CreERT2* [The Jackson Laboratory, #030201 (34)] with *Sphk2*$^{fl/fl}$, *S1pr1*$^{fl/fl}$ (provided by R. Proia, NIH) (47),

or *Spns2*$^{fl/fl}$ (49) mice. Wild-type C57BL/6J mice were purchased from The Jackson Laboratory (#000664). *Sphk2*^{PTECKO}, *Sphk2*^{PTECWT}, and *Pdgfr*β-*CreERT2;Sphk2*$^{fl/fl}$ mice (and their littermate controls) and wild-type mice were on the C57BL/6J background, and the other mice were on a mixed background. Mice were maintained in standard vivarium housing (up to five mice per cage, 12-hour light/dark cycle) on a chow diet, and water was freely available.

Kidney IRI (unilateral and bilateral)

Mice were anesthetized with an intraperitoneal injection of ketamine (120 mg/kg) and xylazine (12 mg/kg) and underwent unilateral (left kidney) or bilateral kidney IRI, as previously described (67, 68). Briefly, unilateral or bilateral flank incision was performed, and either the left pedicle or both renal pedicles were cross clamped for 26 min [wild-type, *Sphk2*^{PTECKO}, *Sphk2*^{PTECWT}, and *Pdgfr*β-*CreERT2;Sphk2*$^{fl/fl}$ (and their littermate controls)], 30 min (*Sphk2*^{PVCKO}, *Sphk2*^{PVCWT}, *S1pr1*^{PVCKO}, and *S1pr1*^{PVCWT}), or 34 min (*Spns2*^{PVCKO} and *Spns2*^{PVCWT}). Tamoxifen was prepared as previously described (69) and intraperitoneally injected (2 mg per mouse) to delete *Sphk2* in *Pdgfr*β-*CreERT2;Sphk2*$^{fl/fl}$ mice (and their littermate controls). Clamp time was optimized for each mouse line based on pilot experiments because susceptibility to kidney IRI is different depending on the genetic background. The clamps were then removed, and the wound was sutured after restoration of blood flow was visually observed. Sham-operated mice underwent the same procedure except that the renal pedicles were not clamped. Mice received buprenorphine sustained release (0.5 mg/kg, sc) as a postoperative analgesic. In unilateral IRI experiments, mice were reanesthetized and subjected to right nephrectomy on day 13, 24 hours before euthanasia to reveal changes in kidney function of the operated, ischemic left kidney assessed by measuring plasma creatinine. In some unilateral IRI experiments, neutral clodronate liposomes or control liposomes (FormuMax Scientific) were intraperitoneally injected (200 μl on day 2 and 100 μl on days 6 and 10 after unilateral IRI) to deplete phagocytic monocytes and macrophages (46). In another subset of experiments, mice underwent unilateral IRI (day 0) and were administered Spns2 inhibitor (SLF1081851, 5 or 10 mg/kg, ip), fingolimod (0.1 or 1 mg/kg, ip), or vehicle (5% hydroxypropyl-β-cyclodextrin) once daily from day 4 to day 13. In bilateral IRI experiments and a subset of unilateral IRI experiments, kidneys were allowed to reperfuse for a period of 24 hours. Mice were euthanized with an overdose of ketamine and xylazine, and blood (400 to 600 μl) was collected from the retroorbital sinus. The kidneys were harvested for histology and RNA extraction. The person performing the surgical procedures (the renal clamp and nephrectomy) had no knowledge of experimental setting including genotype.

Folic acid injection

Male mice were injected with folic acid (250 mg/kg ip in a vehicle of 0.3 M sodium bicarbonate) and euthanized 1 day (AKI model) or 14 days (kidney fibrosis model) later. In some folic acid experiments, mice were administered Spns2 inhibitor (SLF1081851, 5 or 10 mg/kg, ip) or vehicle (5% hydroxypropyl-β-cyclodextrin) once daily from day 4 to day 13. Another subset of mice was followed up to 3 days after injection, and blood was collected from the tail vein on day 2 and day 3.

Cell culture

Perivascular cells and tubular epithelial cells were isolated from the kidneys of male untreated *Sphk2*^{PTECKO}, *Sphk2*^{PVCKO}, and the respective littermate control mice and cultured as previously described (18, 46). In some experiments, *Sphk2*^{PVCWT} and *Sphk2*^{PVCKO} mice underwent unilateral IRI or sham; 6, 24, or 72 hours later, kidney perivascular cells were isolated, and then immediately, mRNA or protein was extracted and analyzed. Human primary kidney perivascular cells (H-6016) and human histiocytic lymphoma cells (U-937 and CRL-1593.2) were purchased from Cell Biologics and American Type Culture Collection, respectively, and cultured according to the manufacturer's protocol. Primary tubular epithelial cells migrate out of the tubules and form a confluent monolayer by days 7 to 10, which was used for experiments. Perivascular cells (passages 3 to 6) were cultured in 100-mm gelatin-coated dishes (for S1P measurement) or in 12-well gelatin-coated plates at a density of 2×10^6 cells per dish or 0.1×10^6 cells per well for 24 hours in the perivascular cell medium containing 10% fetal bovine serum (FBS). Then, cells were washed with phosphate-buffered saline and incubated for 2 hours with FBS-free medium containing 0.5% fatty acid–free bovine serum albumin (BSA) (GoldBio) and stimulated with transforming growth factor–β (10 ng/ml; Thermo Fisher Scientific), LPS (100 ng/ml; Sigma-Aldrich), $Pam_3Cys\text{-}Ser\text{-}(Lys)_4$ (Pam_3CSK_4, 10 ng/ml; InvivoGen), $Pam_2CGDPKHPKSF$ (FSL-1, 10 ng/ml; InvivoGen), or kidney DAMPs (20%) for 2, 6, or 24 hours. Kidney DAMPs were collected from injured (left) kidneys of wild-type mice 24 hours after unilateral IRI under sterile conditions as previously described (45). Supernatants collected from normal kidneys were used as controls. Cytokine and chemokine concentrations in the supernatants were determined using ELISA kits (Thermo Fisher Scientific or R&D Systems). NF-κB activity in the nucleus was quantified as per the manufacturer's protocol (Active Motif). In some experiments, cells were treated with a selective SphK2 inhibitor (SLM6031434) (41) or Spns2 inhibitor (SLF1081851) beginning 2 hours before stimulation. In another subset of experiments, S1P (100 nM; Avanti Polar Lipids) or vehicle (0.4% fatty acid–free BSA) was supplemented to the medium at the same time of LPS stimulation. For gene silencing, small interfering RNAs (siRNAs) (control: D-001810-01, *S1pr1*: J-051684-07/08, *S1pr2*: J-063765-06/08, *S1pr3*: J-040957-05/07, and *Spns2*: J-172375-07/08) from Dharmacon were transfected into perivascular cells at 50 nM using TransIT-siQUEST transfection reagent (Mirus) 48 hours before the experiment following protocols from the manufacturer.

Characterization of SLF1081851 (Spns2 inhibitor)

To determine whether SLF1081851 was efficacious in vivo, SLF1081851 was dissolved in water containing 5% hydroxypropyl-β-cyclodextrin and administered (0, 10, or 30 mg/kg, ip) to 8- to 9-week-old female, C57BL/6 mice. After about 16 hours, blood was drawn from the retro-orbital sinus. Some of the recovered blood was used to determine total lymphocyte numbers using a Heska Element HT5 veterinary blood analyzer, whereas another portion was used to prepare plasma for S1P measurement. Dose response of fingolimod (0, 0.03, 0.1, 0.3, or 1 mg/kg, ip) on total peripheral blood lymphocyte numbers was determined similarly. To determine the IC_{50} of SLF1081851, human histiocytic lymphoma cells (U-937) were collected by centrifugation and resuspended at 1.3×10^6 cells/ml in culture media (RPMI 1640) containing 0.2% fatty acid–free BSA (and 0 to 5 μM SLF1081851). After 3.5

hours at 37°C, medium from 1.5 ml of cell culture was cleared of cells by centrifugation, and after the addition of an internal standard [2.5 pmol of d7S1P (Avanti Polar Lipids)], protein was precipitated by addition of $^{1}/_{10}$ volume of cold 100% trichloroacetic acid, collected by centrifugation, and, after washing with water, the bound S1P was eluted into 0.3 ml of methanol with bath sonication. After clarification by centrifugation, the amounts of recovered S1P were measured by liquid chromatography–mass spectrometry as previously described (30). To assess liver toxicity, plasma AST and ALT were determined using a colorimetric activity assay kit (Cayman Chemical).

Statistical analysis

Statistical analyses were performed using GraphPad Prism 9.0.2 software. All datasets were tested for normality using the Shapiro-Wilk test. All values are expressed as means and SEM. When no error bar is shown, this is because the data were not normally distributed and a nonparametric test was used. Unpaired two-sided Student's *t* test or two-sided Mann-Whitney test was used for comparisons between two groups. One- or two-way analysis of variance (ANOVA), followed by the Tukey's or Sidak's test was used to compare multiple groups. $P < 0.05$ was considered statistically significant.

Supplementary Material

Refer to Web version on PubMed Central for supplementary material.

Acknowledgments:

We thank the UVA Research Histology Core for assistance in preparation of histology slides. The content is solely the responsibility of the authors and does not necessarily represent the official views of the NIH or other funding agencies.

Funding:

Research reported in this publication was supported by the National Institute of Diabetes and Digestive and Kidney Diseases of the NIH (1R01 DK085259 and DK123248 to M.D.O.), by the National Institute of General Medical Sciences of the NIH (1R01 GM121075 to K.R.L. and W.L.S.), by the National Institute of Allergy and Infectious Diseases of the NIH (1R01 AI144026 to W.L.S. and K.R.L.; 1R01 AI085166 and AI123308 to S.R.S.), by the Uehara Memorial Foundation Research Fellowship (to S.T. and T.I.), by Japan Society for the Promotion of Science Overseas Research Fellowships (to S.T. and T.I.), by Kowa Life Science Foundation (to S.T.), by the Ichiro Kanehara Foundation (to S.T.), by the Mochida Memorial Foundation for Medical and Pharmaceutical Research (to S.T.), by MSD Life Science Foundation (to S.T.), by the Uehara Memorial Foundation (to S.T.), by Life Science Foundation of Japan (to S.T.), by the Salt Science Research Foundation, no. 2225 (to ST), by Ben J. Lipps Research Fellowship Grant of the American Society of Nephrology (to N.P.), and by MSTP training grant (5T32GM007267 to E.G.). Data were gathered on an "MBF Bioscience and Zeiss microscope system for stereology and tissue morphology" funded by NIH grant 1S10RR026799-01 (to M.D.O.).

REFERENCES AND NOTES

1. Webster AC, Nagler EV, Morton RL, Masson P, Chronic kidney disease. Lancet 389, 1238–1252 (2017). [PubMed: 27887750]
2. Eckardt KU, Coresh J, Devuyst O, Johnson RJ, Kottgen A, Levey AS, Levin A, Evolving importance of kidney disease: From subspecialty to global health burden. Lancet 382, 158–169 (2013). [PubMed: 23727165]
3. Keith DS, Nichols GA, Gullion CM, Brown JB, Smith DH, Longitudinal follow-up and outcomes among a population with chronic kidney disease in a large managed care organization. Arch. Intern. Med 164, 659–663 (2004). [PubMed: 15037495]

4. Go AS, Chertow GM, Fan D, McCulloch CE, Hsu CY, Chronic kidney disease and the risks of death, cardiovascular events, and hospitalization. N. Engl. J. Med 351, 1296–1305 (2004). [PubMed: 15385656]
5. National Kidney F, KDOQI clinical practice guideline for diabetes and CKD: 2012 update. Am. J. Kidney Dis. 60, 850–886 (2012). [PubMed: 23067652]
6. U. R. D. System, USRDS 2013 annual data report: Atlas of chronic kidney disease and end-stage renal disease in the United States. National Institutes of Health, National Institute of Diabetes and Digestive and Digestive and Kidney Diseases, vol. 2014, (2013).
7. Dixit D, Okuniewska M, Schwab SR, Secrets and lyase: Control of sphingosine 1-phosphate distribution. Immunol. Rev. 289, 173–185 (2019). [PubMed: 30977198]
8. Cartier A, Hla T, Sphingosine 1-phosphate: Lipid signaling in pathology and therapy. Science 366, (2019).
9. Proia RL, Hla T, Emerging biology of sphingosine-1-phosphate: Its role in pathogenesis and therapy. J. Clin. Invest. 125, 1379–1387 (2015). [PubMed: 25831442]
10. Fukuhara S, Simmons S, Kawamura S, Inoue A, Orba Y, Tokudome T, Sunden Y, Arai Y, Moriwaki K, Ishida J, Uemura A, Kiyonari H, Abe T, Fukamizu A, Hirashima M, Sawa H, Aoki J, Ishii M, Mochizuki N, The sphingosine-1-phosphate transporter Spns2 expressed on endothelial cells regulates lymphocyte trafficking in mice. J. Clin. Invest. 122, 1416–1426 (2012). [PubMed: 22406534]
11. Vu TM, Ishizu AN, Foo JC, Toh XR, Zhang F, Whee DM, Torta F, Cazenave-Gassiot A, Matsumura T, Kim S, Toh SES, Suda T, Silver DL, Wenk MR, Nguyen LN, Mfsd2b is essential for the sphingosine-1-phosphate export in erythrocytes and platelets. Nature 550, 524–528 (2017). [PubMed: 29045386]
12. Cohen JA, Barkhof F, Comi G, Hartung HP, Khatri BO, Montalban X, Pelletier J, Capra R, Gallo P, Izquierdo G, Tiel-Wilck K, de Vera A, Jin J, Stites T, Wu S, Aradhye S, Kappos L; TRANSFORMS Study Group, Oral fingolimod or intramuscular interferon for relapsing multiple sclerosis. N. Engl. J. Med. 362, 402–415 (2010). [PubMed: 20089954]
13. Kappos L, Radue EW, O'Connor P, Polman C, Hohlfeld R, Calabresi P, Selmaj K, Agoropoulou C, Leyk M, Zhang-Auberson L, Burtin P; FREEDOMS Study Group, A placebo-controlled trial of oral fingolimod in relapsing multiple sclerosis. N. Engl. J. Med. 362, 387–401 (2010). [PubMed: 20089952]
14. Oo ML, Thangada S, Wu MT, Liu CH, Macdonald TL, Lynch KR, Lin CY, Hla T, Immunosuppressive and anti-angiogenic sphingosine 1-phosphate receptor-1 agonists induce ubiquitinylation and proteasomal degradation of the receptor. J. Biol. Chem. 282, 9082–9089 (2007). [PubMed: 17237497]
15. Schwab SR, Pereira JP, Matloubian M, Xu Y, Huang Y, Cyster JG, Lymphocyte sequestration through S1P lyase inhibition and disruption of S1P gradients. Science 309, 1735–1739 (2005). [PubMed: 16151014]
16. Awad AS, Ye H, Huang L, Li L, Foss FW Jr., Macdonald TL, Lynch KR, Okusa MD, Selective sphingosine 1-phosphate 1 receptor activation reduces ischemia-reperfusion injury in mouse kidney. Am. J. Physiol. Renal Physiol. 290, F1516–F1524 (2006). [PubMed: 16403835]
17. Bajwa A, Jo SK, Ye H, Huang L, Dondeti KR, Rosin DL, Haase VH, Macdonald TL, Lynch KR, Okusa MD, Activation of sphingosine-1-phosphate 1 receptor in the proximal tubule protects against ischemia-reperfusion injury. J. Am. Soc. Nephrol. 21, 955–965 (2010). [PubMed: 20338995]
18. Bajwa A, Rosin DL, Chroscicki P, Lee S, Dondeti K, Ye H, Kinsey GR, Stevens BK, Jobin K, Kenwood BM, Hoehn KL, Lynch KR, Okusa MD, Sphingosine 1-phosphate receptor-1 enhances mitochondrial function and reduces cisplatin-induced tubule injury. J. Am. Soc. Nephrol 26, 908–925 (2015). [PubMed: 25145931]
19. Delbridge MS, Shrestha BM, Raftery AT, El Nahas AM, Haylor J, FTY720 reduces extracellular matrix expansion associated with ischemia-reperfusion induced injury. Transplant. Proc. 39, 2992–2996 (2007). [PubMed: 18089307]

20. Thangada S, Shapiro LH, Silva C, Yamase H, Hla T, Ferrer FA, Treatment with the immunomodulator FTY720 (fingolimod) significantly reduces renal inflammation in murine unilateral ureteral obstruction. J. Urol 191, 1508–1516 (2014). [PubMed: 24679864]
21. Salvadori M, Budde K, Charpentier B, Klempnauer J, Nashan B, Pallardo LM, Eris J, Schena FP, Eisenberger U, Rostaing L, Hmissi A, Aradhye S; FTY720 Study Group, FTY720 versus MMF with cyclosporine in de novo renal transplantation: A 1-year, randomized controlled trial in Europe and Australasia. Am. J. Transplant 6, 2912–2921 (2006). [PubMed: 17061999]
22. Tedesco-Silva H, Pescovitz MD, Cibrik D, Rees MA, Mulgaonkar S, Kahan BD, Gugliuzza KK, Rajagopalan PR, Esmeraldo Rde M, Lord H, Salvadori M, Slade JM; FTY720 Study Group, Randomized controlled trial of FTY720 versus MMF in de novo renal transplantation. Transplantation 82, 1689–1697 (2006). [PubMed: 17198261]
23. Tedesco-Silva H, Szakaly P, Shoker A, Sommerer C, Yoshimura N, Schena FP, Cremer M, Hmissi A, Mayer H, Lang P; FTY720 2218 Clinical Study Group, FTY720 versus mycophenolate mofetil in de novo renal transplantation: Six-month results of a double-blind study. Transplantation 84, 885–892 (2007). [PubMed: 17984842]
24. Camm J, Hla T, Bakshi R, Brinkmann V, Cardiac and vascular effects of fingolimod: Mechanistic basis and clinical implications. Am. Heart J 168, 632–644 (2014). [PubMed: 25440790]
25. Jain N, Bhatti MT, Fingolimod-associated macular edema: Incidence, detection, and management. Neurology 78, 672–680 (2012). [PubMed: 22371414]
26. Schwalm S, Beyer S, Frey H, Haceni R, Grammatikos G, Thomas D, Geisslinger G, Schaefer L, Huwiler A, Pfeilschifter J, Sphingosine kinase-2 deficiency ameliorates kidney fibrosis by up-regulating smad7 in a mouse model of unilateral ureteral obstruction. Am. J. Pathol 187, 2413–2429 (2017). [PubMed: 28807595]
27. Bajwa A, Huang L, Kurmaeva E, Ye H, Dondeti KR, Chroscicki P, Foley LS, Balogun ZA, Alexander KJ, Park H, Lynch KR, Rosin DL, Okusa MD, Sphingosine kinase 2 deficiency attenuates kidney fibrosis via IFN-γ. J. Am. Soc. Nephrol 28, 1145–1161 (2017). [PubMed: 27799486]
28. Yang L, Besschetnova TY, Brooks CR, Shah JV, Bonventre JV, Epithelial cell cycle arrest in G2/M mediates kidney fibrosis after injury. Nat. Med 16, 535–543 (2010). [PubMed: 20436483]
29. Humphreys BD, Lin SL, Kobayashi A, Hudson TE, Nowlin BT, Bonventre JV, Valerius MT, McMahon AP, Duffield JS, Fate tracing reveals the pericyte and not epithelial origin of myofibroblasts in kidney fibrosis. Am. J. Pathol 176, 85–97 (2010). [PubMed: 20008127]
30. Kharel Y, Huang T, Salamon A, Harris TE, Santos WL, Lynch KR, Mechanism of sphingosine 1-phosphate clearance from blood. Biochem. J 477, 925–935 (2020). [PubMed: 32065229]
31. Rankin EB, Tomaszewski JE, Haase VH, Renal cyst development in mice with conditional inactivation of the von Hippel-Lindau tumor suppressor. Cancer Res. 66, 2576–2583 (2006). [PubMed: 16510575]
32. Armulik A, Genove G, Betsholtz C, Pericytes: Developmental, physiological, and pathological perspectives, problems, and promises. Dev. Cell 21, 193–215 (2011). [PubMed: 21839917]
33. Guimaraes-Camboa N, Cattaneo P, Sun Y, Moore-Morris T, Gu Y, Dalton ND, Rockenstein E, Masliah E, Peterson KL, Stallcup WB, Chen J, Evans SM, Pericytes of multiple organs do not behave as mesenchymal stem cells in vivo. Cell. Stem Cell 20, 345–359.e5 (2017). [PubMed: 28111199]
34. Cuervo H, Pereira B, Nadeem T, Lin M, Lee F, Kitajewski J, Lin CS, PDGFRβ-P2A-CreER^{T2} mice: A genetic tool to target pericytes in angiogenesis. Angiogenesis 20, 655–662 (2017). [PubMed: 28752390]
35. Kruse K, Lee QS, Sun Y, Klomp J, Yang X, Huang F, Sun MY, Zhao S, Hong Z, Vogel SM, Shin JW, Leckband DE, Tai LM, Malik AB, Komarova YA, N-cadherin signaling via trio assembles adherens junctions to restrict endothelial permeability. J. Cell Biol 218, 299–316 (2019). [PubMed: 30463880]
36. Rustenhoven J, Drieu A, Mamuladze T, de Lima KA, Dykstra T, Wall M, Papadopoulos Z, Kanamori M, Salvador AF, Baker W, Lemieux M, Da Mesquita S, Cugurra A, Fitzpatrick J, Sviben S, Kossina R, Bayguinov P, Townsend RR, Zhang Q, Erdmann-Gilmore P, Smirnov I,

Lopes MB, Herz J, Kipnis J, Functional characterization of the dural sinuses as a neuroimmune interface. Cell 184, 1000–1016.e27 (2021). [PubMed: 33508229]

37. Dong Y, Zhang Q, Wen J, Chen T, He L, Wang Y, Yin J, Wu R, Xue R, Li S, Fan Y, Wang N, Ischemic duration and frequency determines AKI-to-CKD progression monitored by dynamic changes of tubular biomarkers in IRI mice. Front. Physiol 10, 153 (2019). [PubMed: 30873045]
38. Souza AC, Tsuji T, Baranova IN, Bocharov AV, Wilkins KJ, Street JM, Alvarez-Prats A, Hu X, Eggerman T, Yuen PS, Star RA, TLR4 mutant mice are protected from renal fibrosis and chronic kidney disease progression. Physiol. Rep 3, e12558 (2015). [PubMed: 26416975]
39. Ishani A, Nelson D, Clothier B, Schult T, Nugent S, Greer N, Slinin Y, Ensrud KE, The magnitude of acute serum creatinine increase after cardiac surgery and the risk of chronic kidney disease, progression of kidney disease, and death. Arch. Intern. Med 171, 226–233 (2011). [PubMed: 21325112]
40. Chawla LS, Amdur RL, Amodeo S, Kimmel PL, Palant CE, The severity of acute kidney injury predicts progression to chronic kidney disease. Kidney Int. 79, 1361–1369 (2011). [PubMed: 21430640]
41. Sibley CD, Morris EA, Kharel Y, Brown AM, Huang T, Bevan DR, Lynch KR, Santos WL, Discovery of a small side cavity in sphingosine kinase 2 that enhances inhibitor potency and selectivity. J. Med. Chem 63, 1178–1198 (2020). [PubMed: 31895563]
42. Leaf IA, Nakagawa S, Johnson BG, Cha JJ, Mittelsteadt K, Guckian KM, Gomez IG, Altemeier WA, Duffield JS, Pericyte MyD88 and IRAK4 control inflammatory and fibrotic responses to tissue injury. J. Clin. Invest 127, 321–334 (2017). [PubMed: 27869651]
43. Stark K, Eckart A, Haidari S, Tirniceriu A, Lorenz M, von Bruhl ML, Gartner F, Khandoga AG, Legate KR, Pless R, Hepper I, Lauber K, Walzog B, Massberg S, Capillary and arteriolar pericytes attract innate leukocytes exiting through venules and "instruct" them with pattern-recognition and motility programs. Nat. Immunol 14, 41–51 (2013). [PubMed: 23179077]
44. Tang PM, Nikolic-Paterson DJ, Lan HY, Macrophages: Versatile players in renal inflammation and fibrosis. Nat. Rev. Nephrol 15, 144–158 (2019). [PubMed: 30692665]
45. Campanholle G, Mittelsteadt K, Nakagawa S, Kobayashi A, Lin SL, Gharib SA, Heinecke JW, Hamerman JA, Altemeier WA, Duffield JS, TLR-2/TLR-4 TREM-1 signaling pathway is dispensable in inflammatory myeloid cells during sterile kidney injury. PLOS ONE 8, e68640 (2013). [PubMed: 23844229]
46. Perry HM, Gorldt N, Sung SJ, Huang L, Rudnicka KP, Encarnacion IM, Bajwa A, Tanaka S, Poudel N, Yao J, Rosin DL, Schrader J, Okusa MD, Perivascular $CD73^{+}$ cells attenuate inflammation and interstitial fibrosis in the kidney microenvironment. Am. J. Physiol. Renal Physiol 317, F658–F669 (2019). [PubMed: 31364375]
47. Allende ML, Yamashita T, Proia RL, G-protein-coupled receptor S1P1 acts within endothelial cells to regulate vascular maturation. Blood 102, 3665–3667 (2003). [PubMed: 12869509]
48. Wu H, Kirita Y, Donnelly EL, Humphreys BD, Advantages of single-nucleus over single-cell RNA sequencing of adult kidney: Rare cell types and novel cell states revealed in fibrosis. J. Am. Soc. Nephrol 30, 23–32 (2019). [PubMed: 30510133]
49. Mendoza A, Breart B, Ramos-Perez WD, Pitt LA, Gobert M, Sunkara M, Lafaille JJ, Morris AJ, Schwab SR, The transporter Spns2 is required for secretion of lymph but not plasma sphingosine-1-phosphate. Cell Rep. 2, 1104–1110 (2012). [PubMed: 23103166]
50. Fritzemeier R, Foster D, Peralta A, Payette M, Kharel Y, Huang T, Lynch KR, Santos WL, Discovery of in vivo active sphingosine-1-phosphate transporter (Spns2) inhibitors. J. Med. Chem 65, 7656–7681 (2022). [PubMed: 35609189]
51. Nitzsche A, Poittevin M, Benarab A, Bonnin P, Faraco G, Uchida H, Favre J, Garcia-Bonilla L, Garcia MCL, Leger PL, Therond P, Mathivet T, Autret G, Baudrie V, Couty L, Kono M, Chevallier A, Niazi H, Tharaux PL, Chun J, Schwab SR, Eichmann A, Tavitian B, Proia RL, Charriaut-Marlangue C, Sanchez T, Kubis N, Henrion D, Iadecola C, Hla T, Camerer E, Endothelial S1P1 signaling counteracts infarct expansion in ischemic stroke. Circ. Res 128, 363–382 (2021). [PubMed: 33301355]
52. Zachariah MA, Cyster JG, Neural crest-derived pericytes promote egress of mature thymocytes at the corticomedullary junction. Science 328, 1129–1135 (2010). [PubMed: 20413455]

53. Mendoza A, Fang V, Chen C, Serasinghe M, Verma A, Muller J, Chaluvadi VS, Dustin ML, Hla T, Elemento O, Chipuk JE, Schwab SR, Lymphatic endothelial S1P promotes mitochondrial function and survival in naive T cells. Nature 546, 158–161 (2017). [PubMed: 28538737]
54. Del Gaudio I, Rubinelli L, Sasset L, Wadsack C, Hla T, Di Lorenzo A, Endothelial Spns2 and ApoM regulation of vascular tone and hypertension via sphingosine-1-phosphate. J. Am. Heart Assoc 10, e021261 (2021). [PubMed: 34240614]
55. Zhong L, Jiang X, Zhu Z, Qin H, Dinkins MB, Kong JN, Leanhart S, Wang R, Elsherbini A, Bieberich E, Zhao Y, Wang G, Lipid transporter Spns2 promotes microglia pro-inflammatory activation in response to amyloid-β peptide. Glia 67, 498–511 (2019). [PubMed: 30484906]
56. Blanchard O, Stepanovska B, Starck M, Erhardt M, Romer I, Meyer Zu Heringdorf D, Pfeilschifter J, Zangemeister-Wittke U, Huwiler A, Downregulation of the S1P transporter spinster homology protein 2 (Spns2) exerts an anti-fibrotic and anti-inflammatory effect in human renal proximal tubular epithelial cells. Int. J. Mol. Sci 19, 1498 (2018). [PubMed: 29772789]
57. Galvani S, Sanson M, Blaho VA, Swendeman SL, Obinata H, Conger H, Dahlback B, Kono M, Proia RL, Smith JD, Hla T, HDL-bound sphingosine 1-phosphate acts as a biased agonist for the endothelial cell receptor S1P1 to limit vascular inflammation. Sci. Signal 8, ra79 (2015). [PubMed: 26268607]
58. Perry HM, Huang L, Ye H, Liu C, Sung SJ, Lynch KR, Rosin DL, Bajwa A, Okusa MD, Endothelial sphingosine 1-phosphate receptor-1 mediates protection and recovery from acute kidney injury. J. Am. Soc. Nephrol 27, 3383–3393 (2016). [PubMed: 26961351]
59. Poirier B, Briand V, Kadereit D, Schafer M, Wohlfart P, Philippo MC, Caillaud D, Gouraud L, Grailhe P, Bidouard JP, Trellu M, Muslin AJ, Janiak P, Parkar AA, A G protein-biased S1P1 agonist, SAR247799, protects endothelial cells without affecting lymphocyte numbers. Sci. Signal 13, (2020).
60. Zhao S, Adebiyi MG, Zhang Y, Couturier JP, Fan X, Zhang H, Kellems RE, Lewis DE, Xia Y, Sphingosine-1-phosphate receptor 1 mediates elevated IL-6 signaling to promote chronic inflammation and multitissue damage in sickle cell disease. FASEB J. 32, 2855–2865 (2018). [PubMed: 29401601]
61. Weichand B, Popp R, Dziumbla S, Mora J, Strack E, Elwakeel E, Frank AC, Scholich K, Pierre S, Syed SN, Olesch C, Ringleb J, Oren B, Doring C, Savai R, Jung M, von Knethen A, Levkau B, Fleming I, Weigert A, Brune B, S1PR1 on tumor-associated macrophages promotes lymphangiogenesis and metastasis via NLRP3/IL-1β. J. Exp. Med 214, 2695–2713 (2017). [PubMed: 28739604]
62. Syed SN, Weigert A, Brune B, Sphingosine kinases are involved in macrophage NLRP3 inflammasome transcriptional induction. Int. J. Mol. Sci 21, 4733 (2020). [PubMed: 32630814]
63. Jin J, Lu Z, Li Y, Ru JH, Lopes-Virella MF, Huang Y, LPS and palmitate synergistically stimulate sphingosine kinase 1 and increase sphingosine 1 phosphate in RAW264.7 macrophages. J. Leukoc. Biol 104, 843–853 (2018). [PubMed: 29882996]
64. Colombo E, Di Dario M, Capitolo E, Chaabane L, Newcombe J, Martino G, Farina C, Fingolimod may support neuroprotection via blockade of astrocyte nitric oxide. Ann. Neurol 76, 325–337 (2014). [PubMed: 25043204]
65. Campos LS, Rodriguez YI, Leopoldino AM, Hait NC, Lopez Bergami P, Castro MG, Sanchez ES, Maceyka M, Spiegel S, Alvarez SE, Filamin A expression negatively regulates sphingosine-1-phosphate-induced NF-κB activation in melanoma cells by inhibition of Akt signaling. Mol. Cell. Biol 36, 320–329 (2016). [PubMed: 26552704]
66. Ohkura SI, Usui S, Takashima SI, Takuwa N, Yoshioka K, Okamoto Y, Inagaki Y, Sugimoto N, Kitano T, Takamura M, Wada T, Kaneko S, Takuwa Y, Augmented sphingosine 1 phosphate receptor-1 signaling in cardiac fibroblasts induces cardiac hypertrophy and fibrosis through angiotensin II and interleukin-6. PLOS ONE 12, e0182329 (2017). [PubMed: 28771545]
67. Gigliotti JC, Huang L, Ye H, Bajwa A, Chattrabhuti K, Lee S, Klibanov AL, Kalantari K, Rosin DL, Okusa MD, Ultrasound prevents renal ischemia-reperfusion injury by stimulating the splenic cholinergic anti-inflammatory pathway. J. Am. Soc. Nephrol 24, 1451–1460 (2013). [PubMed: 23907510]

68. Perry HM, Huang L, Wilson RJ, Bajwa A, Sesaki H, Yan Z, Rosin DL, Kashatus DF, Okusa MD, Dynamin-related protein 1 deficiency promotes recovery from AKI. J. Am. Soc. Nephrol 29, 194–206 (2018). [PubMed: 29084809]

69. Jankowski J, Perry HM, Medina CB, Huang L, Yao J, Bajwa A, Lorenz UM, Rosin DL, Ravichandran KS, Isakson BE, Okusa MD, Epithelial and endothelial pannexin1 channels mediate AKI. J. Am. Soc. Nephrol 29, 1887–1899 (2018). [PubMed: 29866797]

70. Inoue T, Abe C, Sung SS, Moscalu S, Jankowski J, Huang L, Ye H, Rosin DL, Guyenet PG, Okusa MD, Vagus nerve stimulation mediates protection from kidney ischemia-reperfusion injury through α7nAChR^{+} splenocytes. J. Clin. Invest 126, 1939–1952 (2016). [PubMed: 27088805]

71. Tanaka S, Abe C, Abbott SBG, Zheng S, Yamaoka Y, Lipsey JE, Skrypnyk NI, Yao J, Inoue T, Nash WT, Stornetta DS, Rosin DL, Stornetta RL, Guyenet PG, Okusa MD, Vagus nerve stimulation activates two distinct neuroimmune circuits converging in the spleen to protect mice from kidney injury. Proc. Natl. Acad. Sci. U.S.A 118, e2021758118 (2021). [PubMed: 33737395]

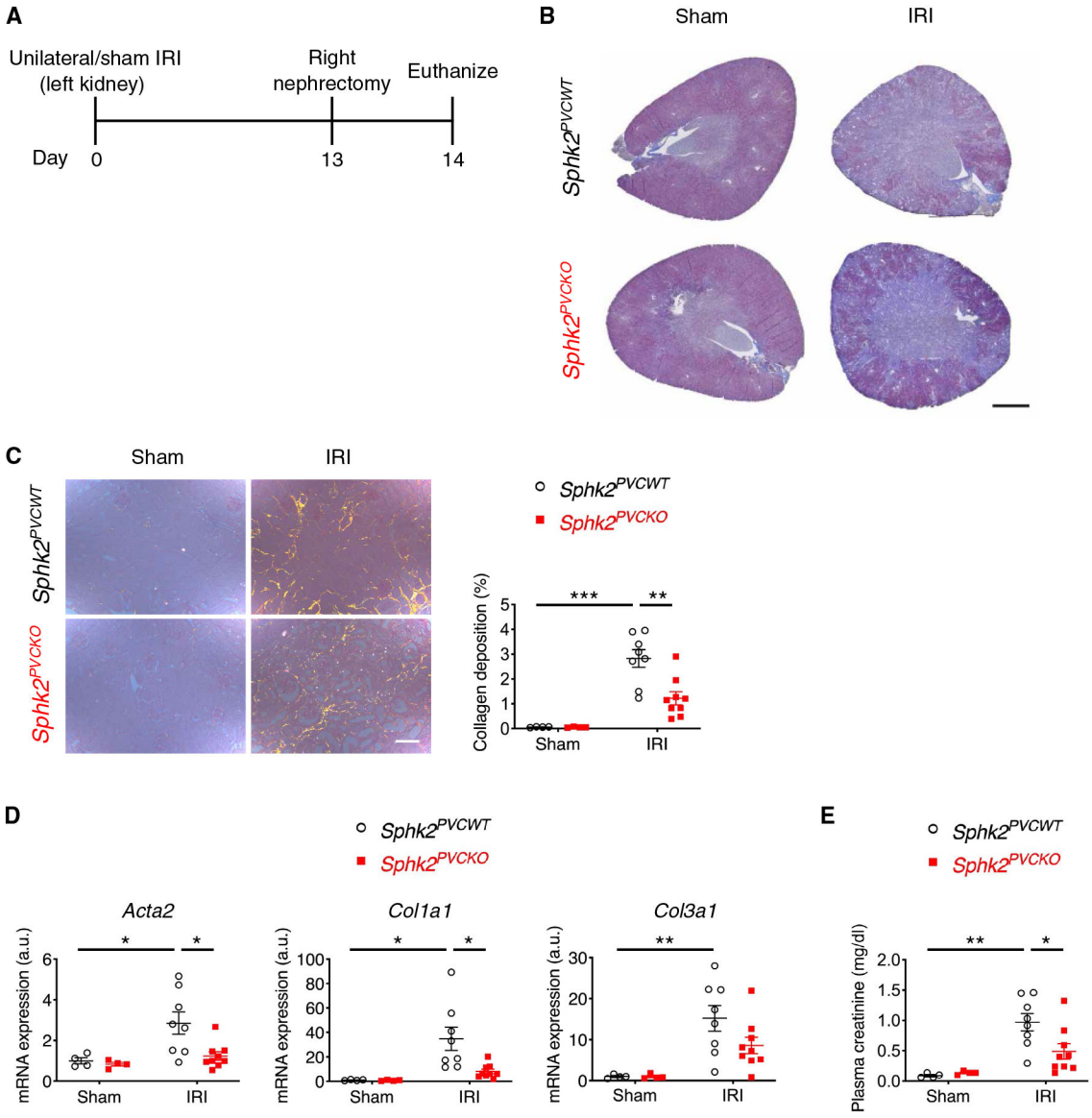

Fig. 1. *Sphk2* deletion in renal perivascular cells ameliorates kidney fibrosis in the unilateral IRI mouse model.

(**A**) Protocol for unilateral IRI to induce kidney fibrosis (for B to E). *Sphk2*^{PVCWT} and *Sphk2*^{PVCKO} mice underwent left renal pedicle clamp for 30 min (day 0) and right nephrectomy at day 13 and were euthanized at day 14. (**B**) Representative Masson's trichrome staining of collagen in kidney sections at day 14. (**C**) Picrosirius red staining of kidney (polarized microscopy, right) with quantification of red/yellow birefringence of mature collagen fibers as a percentage of the total surface area of kidney section at day 14 (left). $n = 4$ to 9 per group. (**D**) *Acta2, Col1a1*, and *Col3a1* transcript expression (from whole kidney) at day 14. $n = 4$ to 9 per group. a.u., arbitrary units. (**E**) Plasma creatinine concentrations at day 14. $n = 4$ to 9 per group. Scale bars, 1 mm (B) and 200 μm (C). Data are represented as means ± SEM. $*P < 0.05$, $**P < 0.01$, and $***P < 0.001$; two-way ANOVA followed by post hoc multiple comparisons test (Tukey's). a.u., arbitrary units.

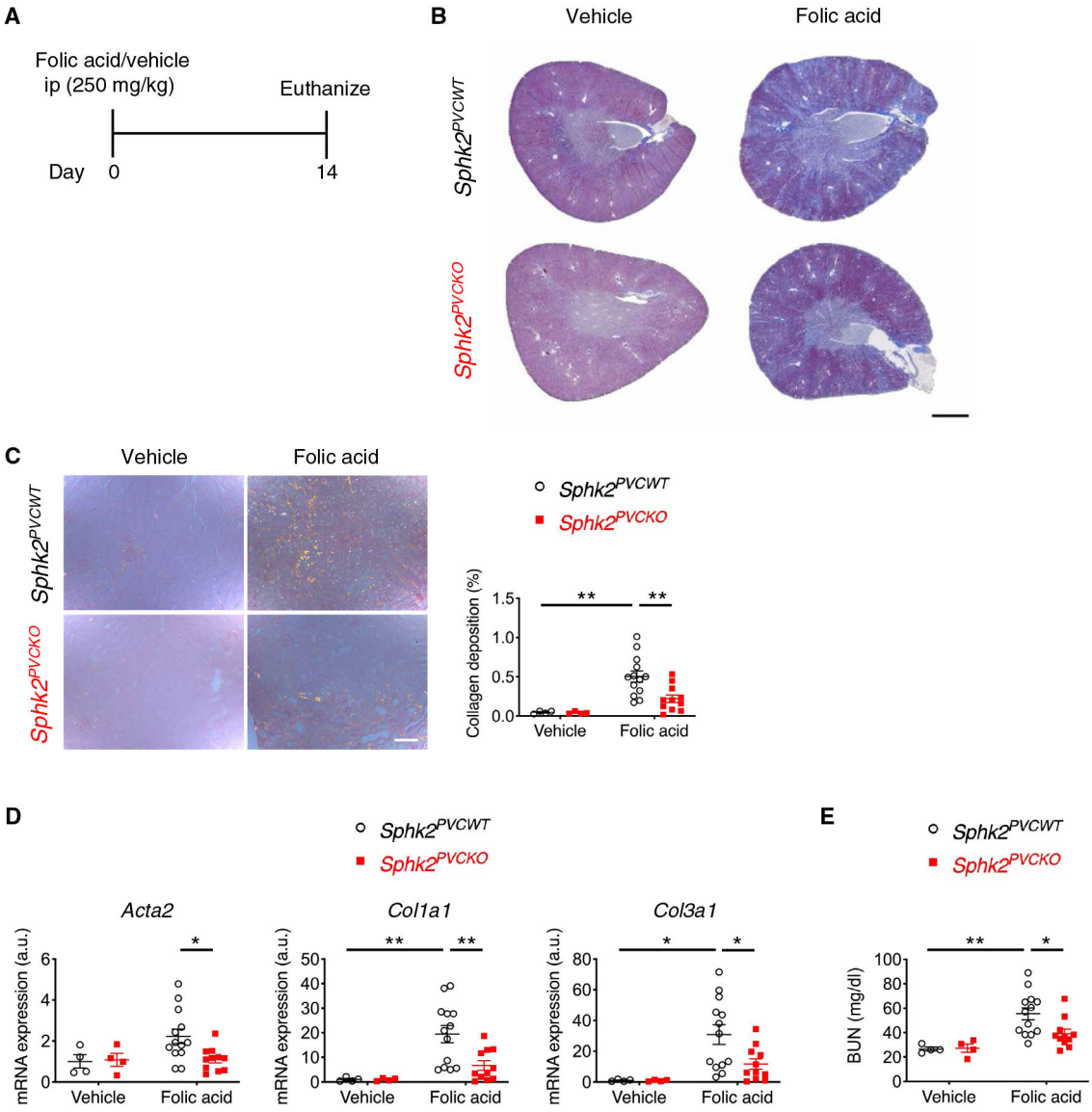

Fig. 2. *Sphk2* deletion in renal perivascular cells ameliorates kidney fibrosis in the folic acid mouse model.

(**A**) Protocol for inducing kidney fibrosis by injecting folic acid (for B to E). *Sphk2*^{PVCWT} and *Sphk2*^{PVCKO} mice were given folic acid (250 mg/kg, ip) and euthanized at day 14. (**B**) Representative Masson's trichrome staining of collagen in kidney sections at day 14. (**C**) Picrosirius red staining of kidney (polarized microscopy) with quantification of red/yellow birefringence of mature collagen fibers as a percentage of the total surface area of kidney section at day 14. $n = 4$ to 13 per group. (**D**) *Acta2, Col1a1*, and *Col3a1* transcript expression (from whole kidney) at day 14. $n = 4$ to 13 per group. (**E**) Blood urea nitrogen (BUN) concentrations at day 14. $n = 4$ to 13 per group. Scale bars, 1 mm (B) and 200 μm (C). Data are represented as means ± SEM. *$P < 0.05$ and **$P < 0.01$; two-way ANOVA followed by post hoc multiple comparisons test (Tukey's).

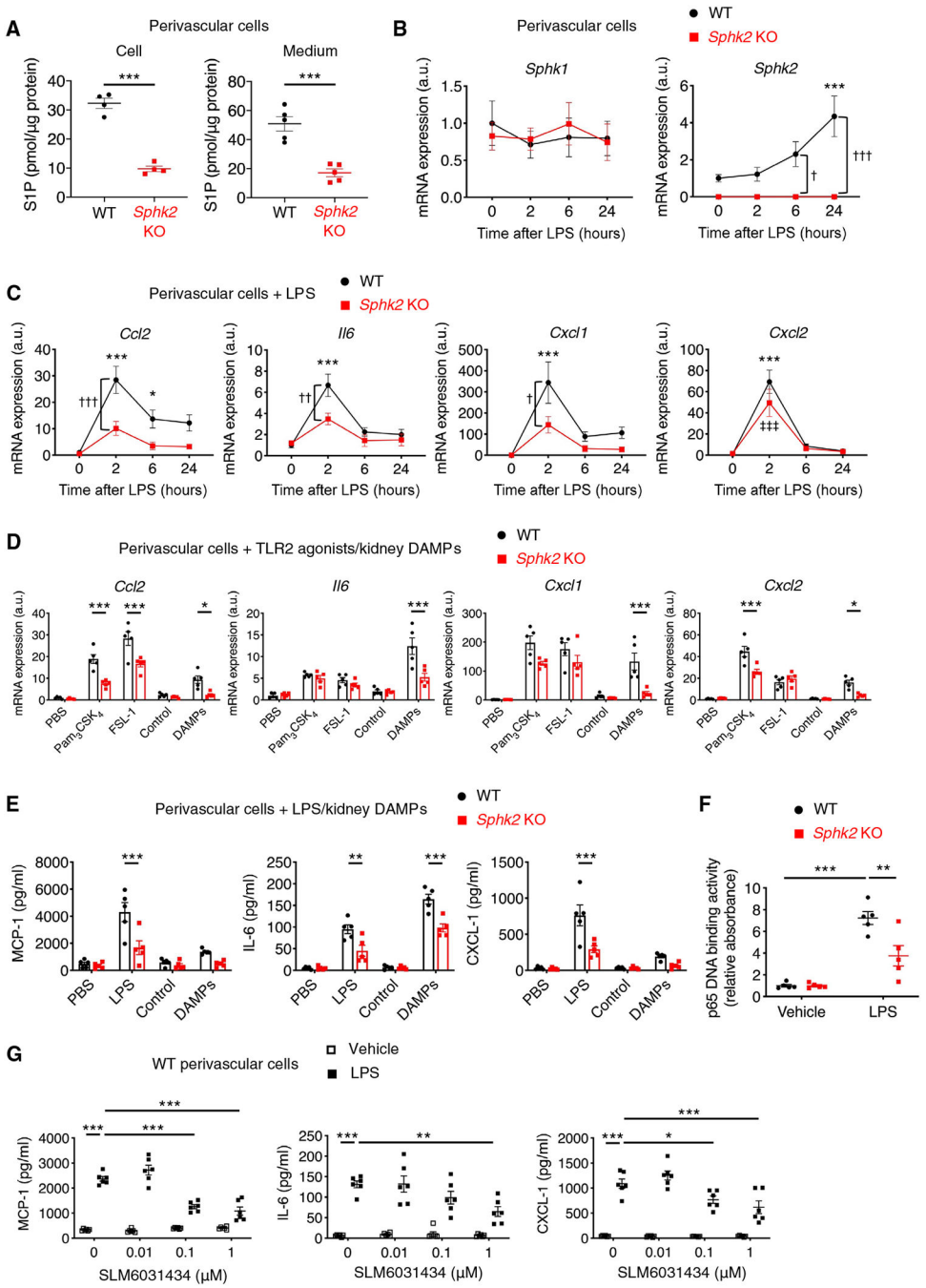

Fig. 3. SphK2 inhibition suppresses inflammatory signaling in mouse perivascular cells.

(**A** to **G**) Experiments were performed using primary kidney perivascular cells isolated from *Sphk2*^{PVCWT} (WT) and *Sphk2*^{PVCKO} [*Sphk2* knockout (KO)] mice. (A) S1P concentrations in perivascular cells and in media. (B and C) Time course of transcript expression of *Sphk1/Sphk2* (B) and proinflammatory cytokines and chemokines (*Ccl2, Il6, Cxcl1*, and *Cxcl2*) after LPS treatment. (D) Transcript expression of *Ccl2, Il6, Cxcl1*, and *Cxcl2* at 2 hours after treatment with TLR2 agonists (Pam_3CSK_4 and FSL-1) or kidney DAMPs. (E) MCP-1, IL-6, and CXCL-1 concentrations in supernatants of kidney perivascular cells treated with LPS

or kidney DAMPs for 24 hours. (F) NF-κB activity at 1 hour after treatment with LPS. (G) Dose response of a selective SphK2 inhibitor (SLM6031434) on MCP-1, IL-6, and CXCL-1 concentrations in supernatants of wild-type kidney perivascular cells at 24 hours after LPS treatment. $n = 4$ to 5 (A), $n = 5$ (B to F), or $n = 6$ (G) per group. Data are represented as means ± SEM. $*P < 0.05$, $**P < 0.01$, and $***P < 0.001$ by unpaired two-sided Student's t test (A) or two-way ANOVA followed by post hoc multiple comparisons test (Tukey's) (D to G). $*P < 0.05$ and $***P < 0.001$ (versus WT at 0 hours); $\dagger P < 0.05$, $\dagger\dagger P < 0.01$, and $\dagger\dagger\dagger P < 0.001$ (WT versus *Sphk2* KO at the same time point); $\ddagger\ddagger\ddagger P < 0.001$ (versus *Sphk2* KO at 0 hours) by two-way ANOVA followed by post hoc multiple comparisons test (Tukey's) (B and C).

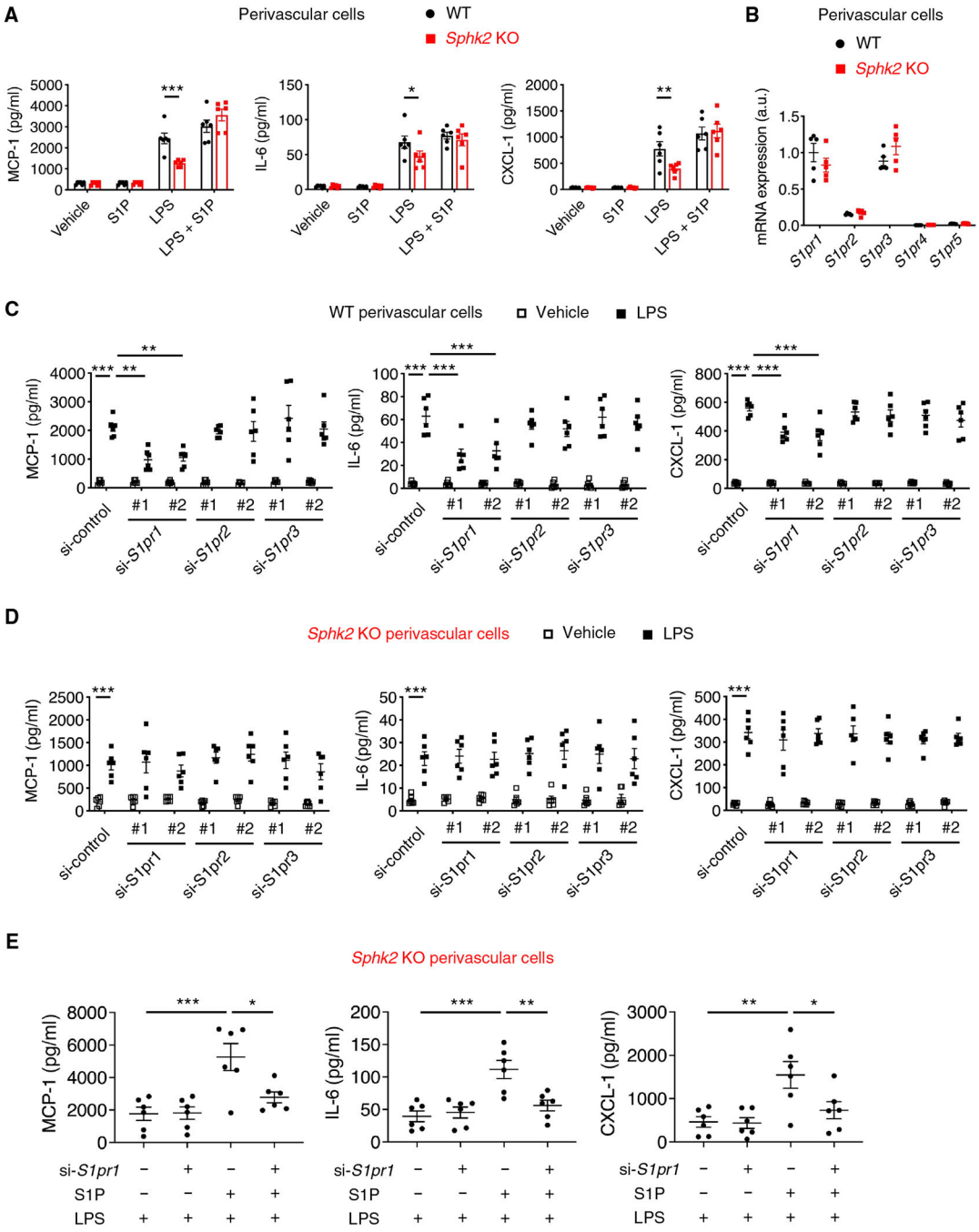

Fig. 4. S1P produced by SphK2 is exported to the extracellular space and binds to S1P1 to enhance inflammatory signaling in perivascular cells.

(**A** to **E**) Experiments were performed using primary kidney perivascular cells isolated from *Sphk2*^{PVCWT} [wild-type (WT)] and *Sphk2*^{PVCKO} (Sphk2 KO) mice. (A) MCP-1, IL-6, and CXCL-1 concentrations in supernatants of primary kidney perivascular cells treated with LPS (100 ng/ml) for 24 hours with or without S1P supplementation (100 nM). (B) *S1pr1-5* transcript expression at baseline. (C and D) MCP-1, IL-6, and CXCL-1 concentrations in supernatants of WT (C) and *Sphk2* KO (D) kidney perivascular cells at 24 hours after treatment with LPS (100 ng/ml). Cells were treated with control, *S1pr1, S1pr2*, or

S1pr3 siRNA before LPS stimulation. (E) MCP-1, IL-6, and CXCL-1 concentrations in supernatants of *Sphk2* KO kidney perivascular cells treated with LPS (100 ng/ml) for 24 hours with or without S1P supplementation (100 nM). Cells were treated with control or *S1pr1* siRNA before LPS stimulation. $n = 6$ (A, C, D, and E), $n = 5$ (B) per group. Data are represented as means ± SEM. $^{*}P < 0.05$, $^{**}P < 0.01$, and $^{***}P < 0.001$ by two-way (A to D) or one-way (E) ANOVA followed by post hoc multiple comparisons test (Tukey's).

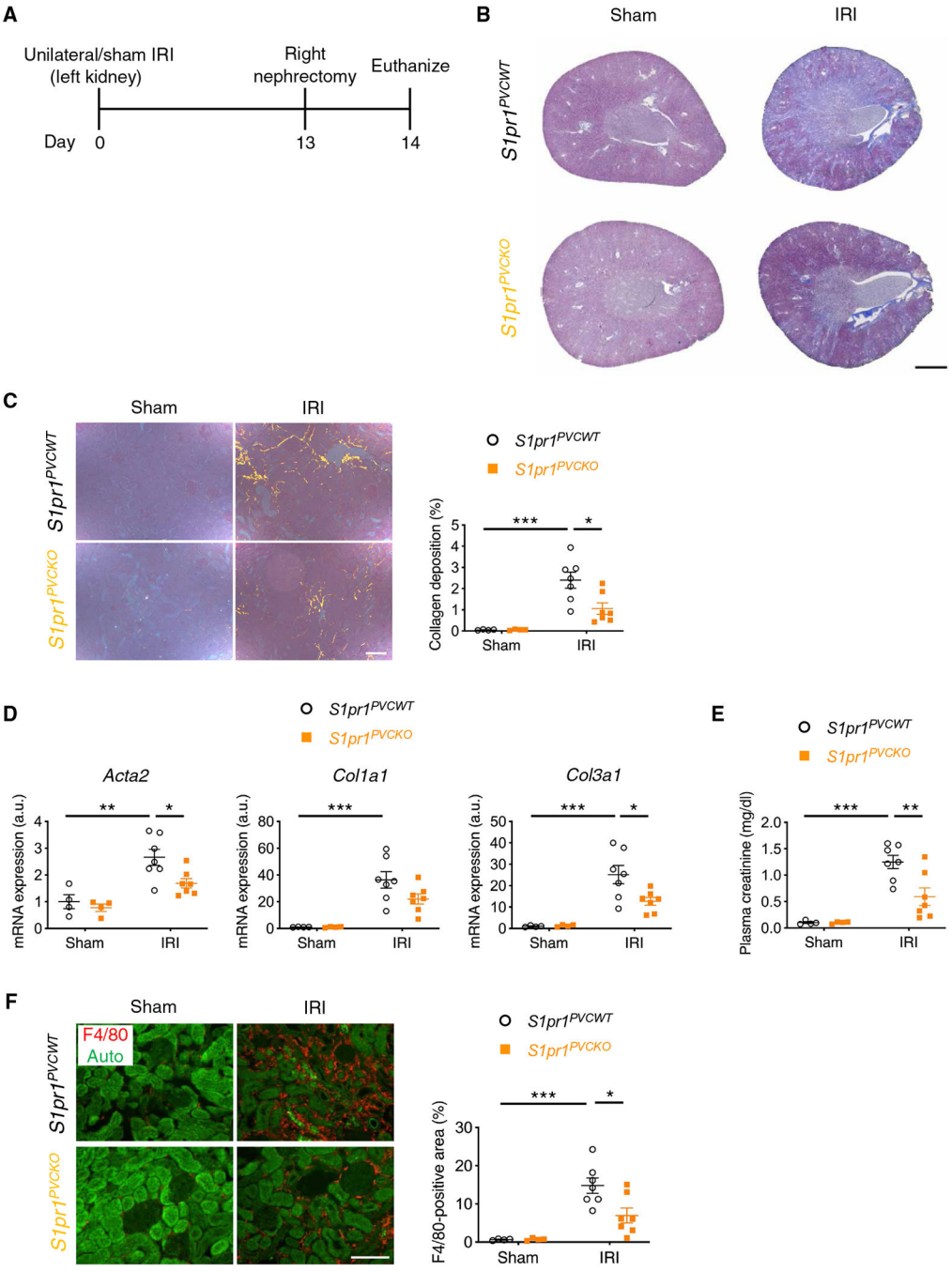

Fig. 5. *S1pr1* deletion in renal perivascular cells ameliorates kidney fibrosis in the unilateral IRI mouse model.

(**A**) Protocol for unilateral IRI to induce kidney fibrosis in mice (for B to F). *S1pr1*^{PVCKO} (*Foxd1-Cre;S1pr1*$^{fl/fl}$) mice, in which *S1pr1* is deleted in kidney perivascular cells, and Cre-negative littermate control (*S1pr1*^{PVCWT}) mice underwent left renal pedicle clamp for 30 min (day 0) and right nephrectomy at day 13 and were euthanized at day 14. (**B**) Representative Masson's trichrome staining of collagen in kidney sections at day 14. (**C**) Picrosirius red staining of kidney (polarized microscopy, left) with quantification of red/yellow birefringence of mature collagen fibers as a percentage of the total surface area

of kidney section at day 14 (right). (**D**) *Acta2, Col1a1*, and *Col3a1* transcript expression (from whole kidney) at day 14. (**E**) Plasma creatinine concentrations at day 14. (**F**) Macrophage staining (F4/80, red, left) of kidney with quantification of F4/80-positive area as a percentage of the total surface area of kidney section at day 14 (right). Auto, autofluorescence (green). Scale bars, 1 mm (B), 200 μm (C), and 100 μm (F). $n = 4$ to 7 per group. Data are represented as means ± SEM. $*P < 0.05$, $**P < 0.01$, and $***P<0.001$; two-way ANOVA followed by post hoc multiple comparisons test (Tukey's).

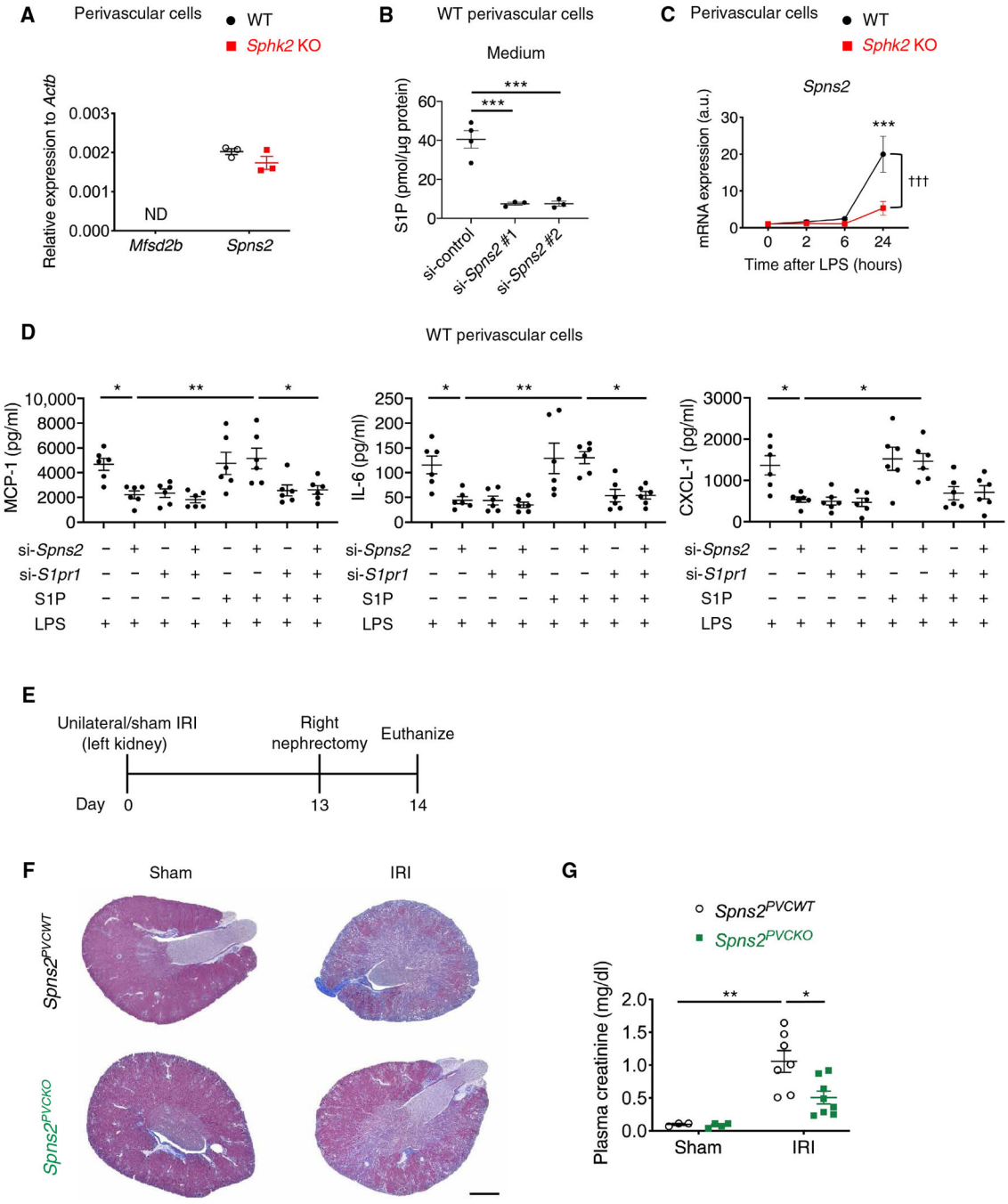

Fig. 6. Spns2 is an S1P transporter expressed in perivascular cells and enhances inflammatory signaling and fibrosis on injury.

(**A**) *Mfsd2b* and *Spns2* transcript expression at baseline in primary kidney perivascular cells isolated from *Sphk2*^{PVCWT} (WT) and *Sphk2*^{PVCKO} (*Sphk2* KO) mice. ND, not detected. (**B**) S1P concentrations in the supernatant of wild-type kidney perivascular cells treated with control or *Spns2* siRNA. (**C**) *Spns2* transcript expression over time after LPS treatment in primary kidney perivascular cells isolated from *Sphk2*^{PVCWT}(WT) and *Sphk2*^{PVCKO} (*Sphk2* KO) mice. (**D**) MCP-1, IL-6, and CXCL-1 concentrations in supernatants of wild-type kidney perivascular cells treated with LPS (100 ng/ml) for 24 hours with or without S1P

supplementation (100 nM). *Spns2* and/or *S1pr1* were knocked down before LPS stimulation. (**E**) Protocol for unilateral IRI to induce kidney fibrosis (for F and G). $Spns2^{PVCKO}$ (*Foxd1-Cre;*$Spns2^{fl/fl}$) mice, in which *Spns2* is deleted in kidney perivascular cells, and Cre-negative littermate control ($Spns2^{PVCWT}$) mice underwent left renal pedicle clamp for 34 min (day 0), right nephrectomy at day 13, and were euthanized at day 14. (**F**) Representative Masson's trichrome staining of collagen in kidney sections at day 14. (**G**) Plasma creatinine concentrations at day 14. Scale bar, 1 mm. $n = 3$ (A), $n = 3$ to 4 (B), $n = 5$ (C), $n = 6$ (D), or $n = 3$ to 8 (E to G) per group. Data are represented as means ± SEM. $^{*}P < 0.05$, $^{**}P < 0.01$, and $^{***}P < 0.001$ by one-way ANOVA followed by post hoc multiple comparisons test (Tukey's) (B and D). $^{***}P < 0.001$ (versus WT at 0 hour); $^{\dagger\dagger\dagger}P < 0.001$ (WT versus *Sphk2* KO) by two-way ANOVA followed by post hoc multiple comparisons test (Tukey's) (C). $^{*}P < 0.05$ and $^{**}P < 0.01$ by two-way ANOVA followed by post hoc multiple comparisons test (Tukey's) (G).

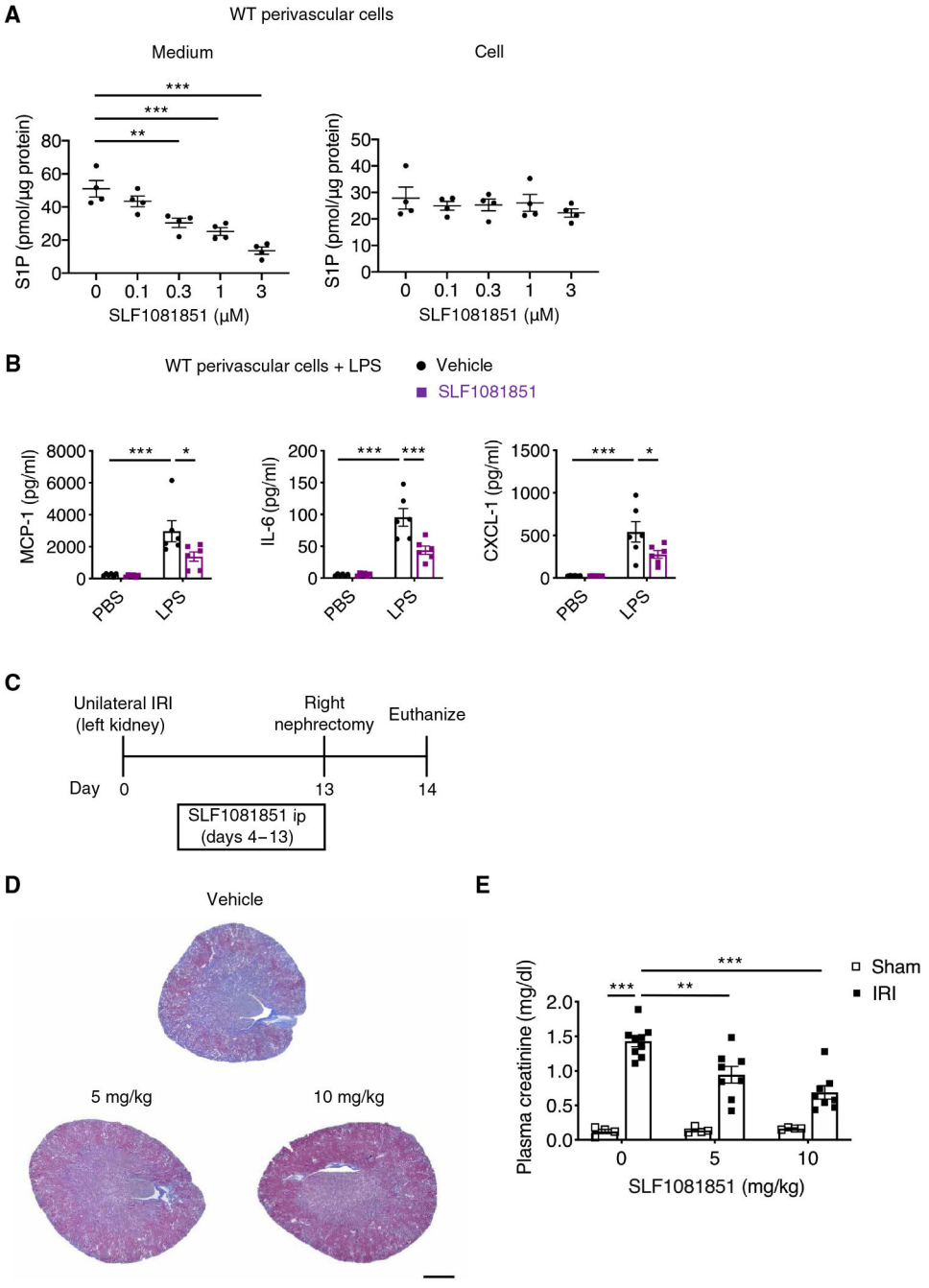

Fig. 7. Pharmacological inhibition of Spns2 suppresses S1P transport and inflammatory signaling in perivascular cells and ameliorates kidney fibrosis.

(**A**) Dose response of a selective Spns2 inhibitor (SLF1081851) on S1P concentrations in wild-type kidney perivascular cells and media. (**B**) MCP-1, IL-6, and CXCL-1 concentrations in supernatants of wild-type kidney perivascular cells treated with LPS (100 ng/ml) for 24 hours. Cells were treated with 3 μM SLF1081851 or vehicle (0.1% fatty acid–free BSA) before stimulation. (**C**) Timeline of experiments (D and E) to investigate the effect of SLF1081851 on kidney fibrosis in wild-type mice. Mice underwent unilateral IRI (day 0) and were administered SLF1081851 (5 or 10 mg/kg, ip) or vehicle

(5% hydroxypropyl-β-cyclodextrin) once daily from day 4 to day 13, followed by right nephrectomy at day 13 and euthanasia at day 14. (**D**) Representative Masson's trichrome staining of collagen in kidney sections at day 14. (**E**) Plasma creatinine concentrations at day 14. Scale bar, 1 mm. $n = 4$ (A), $n = 6$ (B), or $n = 4$ to 9 per group (C to E). Data are represented as means ± SEM. $^{*}P < 0.05$, $^{**}P < 0.01$, and $^{***}P < 0.001$ by one-way (A) or two-way (B and E) ANOVA followed by post hoc multiple comparisons test (Tukey's).